ISTANBUL TECHNICAL UNIVERSITY ★ GRADUATE SCHOOL OF SCIENCE ENGINEERING AND TECHNOLOGY

BUNDLING SHAPE MEMORY ALLOY WIRES TO IMPROVE FREQUENCY RESPONSE AND PAYLOAD LIFTING CAPABILITY

M.Sc. THESIS

Saniye DİNDAR

Department of Mechatronics Engineering

Mechatronics Engineering Programme

JANUARY 2015

ISTANBUL TECHNICAL UNIVERSITY ★ GRADUATE SCHOOL OF SCIENCE
ENGINEERING AND TECHNOLOGY

BUNDLING SHAPE MEMORY ALLOY WIRES TO IMPROVE FREQUENCY RESPONSE AND PAYLOAD LIFTING CAPABILITY

M.Sc. THESIS

Saniye DİNDAR
518121026

Department of Mechatronics Engineering

Mechatronics Engineering Programme

Thesis Advisor: Prof. Dr. Şeniz ERTUĞRUL

JANUARY 2015

İSTANBUL TEKNİK ÜNİVERSİTESİ ★ FEN BİLİMLERİ ENSTİTÜSÜ

FREKANS CEVABININ İYİLEŞTİRİLMESİ VE TAŞINABİLECEK YÜKÜN ARTIRILMASI İÇİN ŞEKİL HAFIZALI ALAŞIMLARIN DEMET OLARAK KULLANILMASI

YÜKSEK LİSANS TEZİ

Saniye DİNDAR
518121026

Mekatronik Mühendisliği Anabilim Dalı

Mekatronik Mühendisliği Programı

Tez Danışmanı: Prof. Dr. Şeniz ERTUĞRUL

OCAK 2015

Saniye Dindar, a **M.Sc** student of ITU **Graduate School of Science Engineering and Technology** student ID **518121026,** successfully defended the **thesis** entitled "**BUNDLING SHAPE MEMORY ALLOY WIRES TO IMPROVE FREQUENCY RESPONSE AND PAYLOAD LIFTING CAPABILITY**", which she prepared after fulfilling the requirements specified in the associated legislations, before the jury whose signatures are below.

Thesis Advisor :   **Prof. Dr. Şeniz ERTUĞRUL**   ....
İstanbul Technical University

Jury Members :   **Doç. Dr. Pınar BOYRAZ**   ....
İstanbul Technical University

Yrd. Doç. Dr. Savaş DİLİBAL   ....
Gedik University

Date of Submission : 12 December 2014
Date of Defense   : 21 January 2015

To my whole family,

FOREWORD

I would like to thank my advisor Prof. Dr. Şeniz Ertuğrul for guiding me to the shortest, practical and simplest way to the solution.
And many thanks to my precious family, has been proud of, for supporting me all along.

October 2014   Saniye DİNDAR
                                                                        (Mechatronics Engineer)

x

TABLE OF CONTENTS

ABBREVIATIONS

DAQ	**:** Data Acquisition
DDDT	: Doğrusal Değişimli Diferansiyel Transformatör
LVDT	: Linear Variable Differential Transformer
PID	**:** Proportional, Integral and Derivative Controller
SMA	**:** Shape Memory Alloy
ŞHA	**:** Şekil Hafızalı Alaşım

LIST OF TABLES

LIST OF FIGURES

BUNDLING SHAPE MEMORY ALLOY WIRES TO IMPROVE FREQUENCY RESPONSE AND PAYLOAD LIFTING CAPABILITY

SUMMARY

Shape memory alloys (SMA), as the name implies, memorize their original shape, which is given at about 700°C. Severe deformations at low temperatures remain until alloy is heated up. In return of heating, alloy remembers and gets its original, pre-deformed shape.

There are two main phases, called martensite and ostenite, causing shape changes of the alloy. Transition between these two phases happens based on temperature changes. Martensite phase occurs when material is cold and that is the phase where deformation takes place. Heating leads material to alter from martensite to ostenite. Then the alloy goes back to its pre-deformed shape by relocating its crystal structure with heat. So, heat is the way of managing of SMA phase transitions which is created either by an outside heat source or by current passing throughout the material. Thus, it is feasible to control position of SMA by controlling the current.

In recent years, the need of lightweight and small actuation technology leads to shape memory alloys to put on the table that have quite promising properties such as high power to mass ratio, easy to establish and noise free working. They provide the opportunity to take conventional actuators' place in many applications; thus encouraging the development of advanced actuators with a noticeable decrease of cost and complexity. While targeting this, there are some drawbacks, such as poor efficiency, low weight lifting capabilities and poor frequency response. In addition, control of SMA becomes a challenge because of hysteresis behavior of the alloy.

Handling couple of SMA drawbacks of it usage as an actuator or an artificial muscle, such as increasing weight lifting capability and improving frequency response, are the main aims of this research.

There are two approaches for a heavier payload that SMA can lift: the easiest way is to use a wider wire. Since thick SMA wire requires more time for cooling after actuation, the wire will be ready seconds afterwards for the next actuation. Consequently, increasing the diameter of the SMA wire results in a good weight lifting capability, in contrast it makes frequency response even worse.

Other approach of improving the payload capability, which is followed in this research, is to bundle an increased the number of SMA wire. The more SMA wire means the more weight lifting capability and the wider surface area. And the fruit of using wider surface area is a shorter cooling time, which results in a better frequency response. All in all, by increasing the number of wire, it is subjected in this research that to get a faster cooling time with the same payload capabilities with a wider SMA wire.

There are three main parts of the experimental setup used in this work: electrical, mechanical and software parts.

Electrical part consists of two SMA wire drivers which were already built for another research and a data acquisition card (DAQ). Wire driver is responsible from sending current to the wire based on the reference voltage received from DAQ card. In order the current to follow the reference value, a PI control was implemented. Controller gains are defined to provide 1 amperes output in return for a 10 volts input. The driver has a closed loop so the output, which is SMA wire actuation current, that follow the reference. However, the loop is closed within the driver and it is not sending back any current feedback to software. Instead, wire driver sends voltage drop value on the SMA wire to data acquisition card as a feedback. Since current value is already known, which is 1/10 of the reference value, it is easy to calculate wire resistance in software by dividing voltage drop value to current value. DAQ card is responsible from acquiring reference voltage data from software and send them to SMA wire drivers. In addition, it delivers voltage drop value from driver card to software.

Mechanical part comprises SMA wires lifting a load (150 gr) and a LVDT (Linear Variable Differential Transformer) to measure displacement of load. Load is placed on a vertical linear guide and core of LVDT is mounted on load. When SMA wire is actuated, it causes the load to displace which in turn leads to core displacement so that LVDT can measure and sends the position data to software. Respectively, two SMA wires with 76 μm diameter, one wire with 100 μm diameter and one wire with 150 μm diameter is screwed carrying same load, 150 gr. Wire length is same for three wires, 30 cm.

Software part built within LabVIEW, using graphical interface, and has two analog outputs: powering up LVDT and sending reference voltage value to the SMA wire driver via DAQ card and two analog inputs: reading position and voltage drop value of SMA. By utilizing these analog inputs and outputs, a sine wave signal at different frequencies (between 0.1 Hz and 7 Hz) is sent as reference signal to the driver. And Bode graph is plotted for three wires with different diameter to compare their frequency responses.

Input signal magnitudes are chosen based on the approximate current value for 1 second given in the manufacturer website.

Open loop and closed loop tests were carried out and open loop results show that,

- Increasing the diameter of the wire results in a slow actuation, since the wire needs more time to cool down.

- For heavier payloads, gain is increasing which means displacement of load becomes longer. However, as a drawback, the heavier the load leads to the larger delays.

- An SMA wire with 76 μm diameter can carry 80 gr load. Doubling the number of the wire increases the payload lifting capability to 160 gr which is higher than 100 μm wire's weight lifting capability. On the other hand, 76 μm wire needs 0.8 second to cool down which is 72% of cooling time of 100 μm wire and 40% cooling time of 150 μm wire. Even 24 μm widening of the wire results in about 30% slower cooling time, which is more obvious at relatively high frequencies.

- Phase delay is 180 degree at 5 Hz for 76 μm wire, 2 Hz for 100 μm wire under 150 gr loading. For the same load, 150 μm wire displaces the load 0.05 mm at 1.2 Hz. Since the wires are twofold, the variation of wire length is actually double of these displacements. Bearing mind that the narrow bandwidth of SMA wires, widening the diameter of SMA wire ends up with a drastically reduced bandwidth.

- For a 0.2 Hz input signal, displacement of the load, which is 150 gr, is 4.3 mm for 76 μm wire, 5 mm for 100 μm wire and 0.8 mm for 150 μm wire. Using about 300 gr payload instead of 150 gr leads 150 μm SMA wire to displace 1.6 mm instead of 0.8 mm.

- Two SMA wires with 76 μm diameters have the same payload lifting capability with one SMA wire with 100 μm diameter. In addition, as mentioned before, two 76 μm SMA wires are about 30% faster than 100 μm SMA wire. Additionally, in theory, it requires two more SMA wires with 76 μm to have the same weight lifting capability with one SMA wire with 150 μm diameter.

On the other hand, outcomes of the closing the control loop are;

- Controller makes the SMA wire contract faster. Since the controller first starts with maximum current to contract the wire rapidly, then decreases the actuation current while the error becomes smaller. Because of the fact that, no current flows during cooling cycle; closed loop control has no influence on cooling.

- In open loop experiments, at 0.2 hertz, 76 μm and 100 μm wires respond to input signal with about 50 degrees of delay. 150 μm wire has a delay about 70 degrees. Closed loop control is eliminated these delays and the all three wires can follow the sine input without any delay at 0.2 hertz.

- Phase delays occuring at 0.2 hertz in case of open loop experiments takes place at about 2 hertz for the closed loop controlled experiments.

- Absolute gain is less than 0.5 for 76 μm and 100 μm wires and almost zero for 150 μm at 1 hertz. At the same frequency, it is about 1 for 76 μm and 100 μm wires and 0.3 for 150 μm at 1 hertz. It can be concluded that, closed loop control of the wires is quite beneficial for both pursuing input signal and displacement of the load.

- Bundling the wires is very effective to accelerate the response and makes evident difference in open loop experiments.

- In closed loop experiments, for small increase in diameter of the wire, bundling does not differ much. However, in case of 76 μm and 150 μm wires, instead of doubling diameter of the wire, it would be more useful, especially for longer displacement at high frequencies, to use 4x76 μm wires in parallel to carry the same load. Since 150 μm wire has a 320 gr payload capability and it is 80 gr for the 76 μm wire.

- Payload has an effect on displacement in open loop experiments but closed loop controlled wire does almost not effected from the load.

Usage of SMA wires in biomedical applications such as artificial muscle, instead of using a thicker wire, it is the most efficient way to bundle the increased the number of thinner wire in order to obtain a faster and powerful muscle. Mechanically parallel bundled SMA wires are more effective than one wire bundled using pulleys, that is, mechanically serial mounted. Since, in case of a damage of a wire does not make the whole actuator or muscle out of use.

FREKANS CEVABININ İYİLEŞTİRİLMESİ VE TAŞINABİLECEK YÜKÜN ARTIRILMASI İÇİN ŞEKİL HAFIZALI ALAŞIMLARIN DEMET OLARAK KULLANILMASI

ÖZET

Şekil hafızalı alaşımlar (ŞHA), adından da anlaşılacağı üzere, yaklaşık 700°C'de verilmiş, ilk şekillerini hatırlayan alaşımlardır. Alaşım, elastik olmayan ve bir limite kadar olan şekil değişimlerini aynen korur. Fakat ısıtıldığında, gerçekleşen bu deformasyonlar ortadan kaybolur ve alaşım ilk şeklini alır.

Alaşımın, martenzit ve östenit olarak adlandırılan ve şekil değişimlerine sebep olan iki ana fazı bulunmaktadır. Bu iki ana faz arasındaki geçişler sıcaklık değişimiyle sağlanır. Martenzit fazı, malzeme soğukken içinde bulunduğu fazdır ve malzeme bu fazda deforme edilir. Malzemenin ısıtılmasıyla, martenzit fazından östenit fazına geçiş başlar. Östenit fazında ise, malzemenin kristal yapısı ilk halini alır ve malzeme deformasyondan önceki şekline dönmüş olur. Dolayısıyla, alaşımın şeklini değiştirmenin yolu, dışardan bir ısı kaynağıyla ya da malzemenin içinden akım geçirerek malzemeyi ısıtmaktır. Bu da, alaşımın içinden geçen akımı kontrol ederek malzemenin şeklini kontrol etme olanağı sağlar.

Son yıllarda, hafif ve küçük eyleyici teknolojisi gereksinimi, şekil hafızalı alaşımların da öne çıkmasına olanak sağladı. Bu alaşımlar, gürültüsüz çalışma, istenilen ebatta hazırlanabilme, kütlesine oranla yüksek güç sağlayabilme gibi önemli avantajlara sahiptir. Ayrıca fiyatının uygun olması ve basit bir yapıya sahip olması da avantajları arasındadır. En önemli dezavantajlarından bazıları ise, verimliliğinin düşük olması, çalışabildiği frekans aralığının dar olması ve düşük yük taşıma kapasitesidir, bununla birlikte gösteridiği histerizis davranış, alaşmın kontrolünü zorlaştırmaktadır.

Yapay kas veya kas benzeri eyleyiciler gibi biyomedikal ve robotik alanlarında kullanılabilmesi için, bu dezavantajlardan bazılarını ortadan kaldırmak amacıyla; taşınabilecek yükü, frekans cevabını kötüleştirmeden artırmak bu çalışmanın hedefini oluşturmaktadır.

Bu doğrultuda, iki temel yaklaşım baz alınabilir: ilki, tel sayısını artırmak taşınabilecek yük kapasitesini de artırmaktadır. Fakat bu, aynı zamanda daha fazla ısı ve ısıdaki artışa nispeten daha küçük bir yüzey alanı genişlemesi olduğundan, soğuma süresi artacak ve tellerde, bir sonraki etkinleştirme için daha fazla gecikmeye neden olacaktır. Dolayısıyla, frekans cevabı kötüleşecektir.

Taşınabilecek yükün artırılmasının bir diğer yolu, aynı zamanda bu çalışmada da izlenen yol, ise küçük çaplı alaşım teli sayısını artırmaktır. Tel sayısının artırılması kaldırılabilecek yükün artırılması demek olduğu gibi, aynı zamanda daha geniş yüzey alanı demektir. Bu da daha kısa soğuma süresi ve daha iyi bir frekans cevabı olarak alaşımın davranışına yansımaktadır. Bu çalışmada da incelenen, ince tellerin demet haline getirilerek daha fazla yükü frekans cevabını kötüleştirmeden kaldırabilmesini sağlamaktır.

Bu çalışma, mekanik, elektronik ve yazılım kısımları olmak üzere, üç ana kısımdan oluşmaktadır.

Elektronik kısmında, daha önce başka bir çalışmada tasarlanmış ve kullanılmış olan, iki şekil hafızalı alaşım sürücü devresi ve bir tane veri toplama kartı bulunmaktadır. Tel sürücü, veri toplama kartından gelen sinyali referans alarak bir akım çıkışı üretir ve bu akımla teli sürer. Teli gönderilen akımın referans sinyalini takip edebilmesi için, devre üzerinde bir PI kontrol gerçekleştirilmiştir. Devre çıkışı, 10 volt girişe karşılık, 1 amper çıkış üretmektedir, yani çıkışın girişe oranı 1/10'dur. Her ne kadar devre kendi içerisinde kapalı çevrim çalışsa da yazılıma akım takibi konusunda herhangi bir geri besleme gelmediğinden genel olarak açık çevrim çalışmaktadır. Akım bilgisi geri besleme olarak yazılıma gönderilmek yerine, tel üzerindeki gerilim düşümü kart tarafından algılanmakta ve yazılıma gönderilmektedir. Bunun yanısıra, referans sinyali de yazılım tarafından belirlendiğinden ve tele gönderilen akım bu sinyalin 1/10'u olduğundan, bu iki verinin birbirine bölünmesiyle telin direnci hesaplanabilmektedir. Elektronik kısmının bir diğer elemanı olan veri toplama kartı ise, konum okuyucudan aldığı konum bilgisini ve tel üzerindeki gerilim düşümü bilgisini yazılıma göndermekle sorumludur. Ayrıca, akım referans sinyalini de tel sürücüye iletmekle görevlidir.

Mekanik kısım, şekil hafızalı alaşım tellerinden, 150 gramlık bir yükten ve yükün konumunu ölçmek için kullanılmış olan, doğrusal değişimli diferansiyel transformatörden (DDDT) oluşmaktadır. Yük, dikey konumlandırılmış tellerin ucuna bağlı olup, diferansiyel transformatöre de mekanik olarak monte edilmiştir. Dolayısıyla, alaşım etkinleştirildiğinde, telin boyu değişecek, yük hareket edecektir. Konumu değişen yük ile konum ölçer birlikte hareket ettiğinden, yükün son konumu konum ölçer tarafından okunmuş olacaktır. Kullanılan yük 150 gram olup, sırasıyla iki adet 76 µm, bir adet 100 µm ve bir adet 150 µm çaplı tellerin ucuna bağlanmıştır. Tellerin, her birinin boyu yaklaşık 30 cm'dir.

Sistemin yazılımı, National Instruments firması tarafından piyasaya sürülmüş olan, LabVIEW ortamında grafik arayüz kullanılarak hazırlanmıştır. DDDT'yi beslemek ve referans voltajını göndermek için iki analog çıkış; konumu ve tel üzerindeki voltaj düşüşünü okumak için de iki analog giriş kullanılmıştır. Bu giriş ve çıkışlar kullanılarak, farklı frekanslardaki (0.1-7 Hz arasında) sinüs sinyalleri, tel sürücüye referans sinyali olarak gönderilmiştir. Yükün konum değişimi, sistemin çıkışı olarak okunmuş ve hem açık çevrim, hem de kapalı çevrimde bode grafikleri elde edilmiştir. Her tel için bu grafikler hazırlanmış ve frekans cevaplarının karşılaştırılması yapılmıştır.

Giriş sinyali genlikleri, teller farklı akımlarda etkinleştirildiğinden, üretici firmanın vermiş olduğu verilere göre belirlenmiştir.

Açık çevrim frekans cevabı sonuçları aşağıdaki gibidir:

- Telin çapının genişletilmesi, telin soğuması daha çok zaman aldığından, daha yavaş bir etkinleşmeye neden olmuştur.

- Daha ağır yüklerde, yükün yer değiştirmesi daha fazla olmuştur. Fakat buna bağlı olarak, daha fazla yük, sisteme daha fazla gecikme getirmiştir.

- 76 µm çaplı bir tel, 80 gram yük taşıyabilmektedir. Tel sayısı ikiye katlandığında taşınabilecek yük de 160 grama çıktığından, 150 gram taşıyabilen 100 µm'lik bir alaşım telinden daha fazla yük taşınmış olacaktır. Diğer yandan, 76 µm'lik tel soğumak için 0.8 saniyeye ihtiyaç duymaktadır,

ki bu süre, 100 μm'lik telin soğuma süresinin % 72'sini, 150 μm'lik telin soğuma süresinin ise % 40'ını teşkil etmektedir. Çaptaki, 24 μm'lik bir artış bile, yüksek frekanslarda daha belirginleşen, yaklaşık % 30'luk bir geç soğumayla sonuçlanmaktadır.

- Fazda 180 derecelik bir gecikme, 76 μm'lik telde 5 Hz'de, 100 μm çaplı telde 2 Hz'de gerçekleşmektedir. 150 μm çaplı telde ise 1.2 Hz'de yük, 0.05 mm yer değiştirmiştir. Tellerin boylarındaki değişim ise, tel ikiye katlanarak kullanıldığından, bu yer değiştirmelerin iki katıdır. Dolayısıyla çapı genişletmek, zaten dar olan, telin çalışabildiği frekans aralığını da daraltmaktadır.

- 2 Hz'lik bir giriş sinyaline karşılık, ucunda 150 gramlık yük bağlanmış olan tellerden, 76 μm'lik iki tel, yükün konumunu 4.3 mm, 100 μm'lik tek tel 5 mm ve 150 μm'lik tel ise 0.8 mm değiştirmiştir. Yaklaşık 300 gramlık bir yük kullanılması durumunda ise, 150 μm'lik tel 0.8 mm yerine 1.6 mm yer değiştirmiştir ki bu da yük arttıkça konum değişiminin belli bir limite kadar arttığının göstergesidir.

- Daha önce de belirtildiği gibi, iki 76 μm'lik ŞHA teli, tek 100 μm'lik ŞHA telinin taşıyabileceği yükü taşımış ve yüksek frekanslarda daha hızlı soğuma gerçekleştirmiştir. Teorik olarak, 76 μm'lik telin, 150 μm'lik telin taşıyabileceği maksimum yükü taşıyabilmesi için ise, iki adet daha 76 μm'lik ŞHA teline ihtiyaç vardır.

Teller, kapalı çevrim kontrol edildiğinde ise sonuçlar aşağıdaki gibi olmaktadır:

- Kontrolör, tellerin daha hızlı ısınmasını sağladığından ve hata azaldıkça etkinleştirme akımını da azalttığından, tellerin kasılma süresi kısalmıştır. Soğuma süresince herhangi bir akım gönderilmediğinden, kontrolörün soğuma kısmında etkisi olmamıştır.

- Açık çevrimde, 0.2 hertz frekansta, 76 μm ve 100 μm teller yaklaşık 50 derecelik bir gecikme ile kasılmışlardır. Aynı durum 150 μm'lik telde 70 derecelik gecikmeyle gerçekleşmiştir. Çevrim kapalı hale getirildiğinde ise, bu gecikmeler 0.2 hertz yerine 2 hertzde gerçekleşmiştir. Kapalı çevrimde, 0.2 hertz frekansında herhangi bir gecikme olmadan, teller, giriş sinyalini takip etmiştir.

- 1 hertzde, mutlak genlik değeri, 76 ve 100 μm çaplı teller için 0.5'ten az iken, 150 μm çaplı tel için bu değer 0 civarındadır. Çevrim kapalı hale getirildiğinde, genlikler oranı ince teller için 0.5 civarından 1'e yükselirken, 0 civarı olan kalın telin genlikler oranı 0.3'e yükselmiştir.

- Kapalı çevrim kontrollü telin kalınlığının az bir miktar artırılması frekans cevabını etkilemezken, çap iki katına çıkarıldığında, demet olarak kullanım hem genlik değerini iyileştirmekte hem de gecikmeyi azaltmaktadır. Fakat 76 μm çaplı telin, iki katı çaptaki tel ile aynı yükü kaldırabilmesi için, demetteki tel sayısını da 4'e çıkarmak gerekmektedir.

- Yükün etkisi, genliği artırma olarak açık çevrimde hissedilirken, kapalı çevrimde etkisi oldukça azdır.

Şekil hafızalı alaşımların, yapay kas gibi biyomedikal uygulamalarda kullanımında, kalın tel yerine, ince tellerin demet olarak kullanılmasının, frekans cevabını kötüleştirmeden daha fazla yük taşıyabilmek adına, daha efektif olduğu sonucuna

varılmıştır. Demet haline getirilen tellerin, makaralarla paralelleştirmek yerine, mekanik olarak paralel kullanımı, eyleyicinin uzun ömürlü olması açısından, faydalı olduğu da varılan sonuçlar arasındadır.

1. INTRODUCTION

Shape memory alloys, as mentioned before, memorizes their original shape. The term shape memory refers to ability of certain materials to "remember" a shape, even after rather severe deformations: once deformed at low temperatures, these materials will stay deformed until heated, whereupon they will return to their original, pre-deformed "learned" shape [10]. These unique materials can be formed into any shape such as wire or spring under quite high temperatures, about 700°C for 30 minutes.

There are many types of shape memory alloys composed of copper, aluminium, nickel, gold, iron and zinc etc [34]. Nitinol, which is made of % 55-56 Nickel and %45-46 Titanium and found by Naval Ordnance Laboratory, is one of the most common and powerful one. Tiny changes in the material percentages make significant influences in the material properties such as elasticity used by orthodontics or shape memory effect useful for actuators.

As it is shown in figure 1.1, many of the other materials have one type of crystal structure but SMAs have two different crystal structures which is called martensite, cold phase, and ostenite, hot phase.
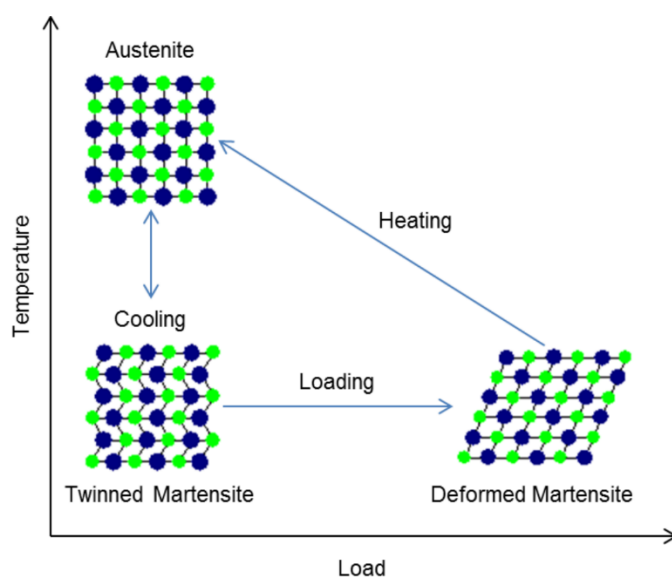

Figure 1.1 : Shape memory effect [4].

In case of martensite phase, material is generally deformable and super elastic. In the ostenite phase case, material is stiffer and high yield point.

The shape memory effect takes place when the material is heated above a certain temperature alterating its phase from martensite to austenite. The transition occurs between martensite phase, when material is cold and ostenite phase when material is hot. These phase changes lead to dimention and shape alteration in the material. Heating is caused either by an outside heat source or by current passing throughout the material, resulting in joule heating. Rather than heat source, current can be controlled for phase changes of the material. Heating the material can be controlled however cooling it is quite hard to control. Common cooling way is just to wait for heat transmission from SMA material to ambient without applying any actuation current.

The term shape memory describes that the material has the ability to go back to a preset shape when heated after deforming the material. There are five significant functions SMA can deliver:

- Free Recovery means displacement without work. This function generally used in control devices and relay mechanisms and especially stents.

- Constrained recovery means that material is not allowed to displace generating high amount of stresses. Couplings and connectors for machinery are main equipment for this function.

- Usage of SMA as actuator, it produces force along with displacement which delivers the advantage of lightweight and noiseless applications.

- Superelasticity provides high elastic deformation to SMA. Eyeglass frames or stents are the example of superelasticity function usage of SMA.

- High damping capacity of martensite phase used in golf wedges, putters and clubs include spin on the ball with a greater control [13].

Since SMAs are noise free, easy to mount, miniaturizable and have high power to mass ratio, they provides opportunity to take conventional actuators' place; thus encouraging the development of advanced actuators with a noticeable decrease of cost and complexity. Expecially lightweight property of SMA material is the best fit for light robotics. On the other hand, their low efficiency, narrow bandwidth are the main drawbacks. In addition, many parameters of SMA wire such as strain, position

or resistance are dependent on temperature, which is quite difficult to measure cause of limited physical properties.

1.1 Purpose of Thesis

One of the most promising new actuator technologies developed in the last few years are the actuators employing shape memory properties. Actuators based on shape memory alloys (SMA) have a high power to weight ratio and have found applications in many areas including micromechatronics and light robotics [8].

In this research, the main objective is to use SMA wires as actuator, which has the great advantage of drastically reduced weight of the actuator and no need of extra components such as gearbox etc. To pursue this aim, it is required to increase the weight lifting capability of SMA wire. Increasing the diameter or the number of the wire are the options to increase payload to weight ratio.

Second goal of this work is to make faster SMA wire. The way of achieving it is to shorten cooling time of the wire. The wider surface area means the more heat dissipation, which is in return cause SMA to cool faster. Instead of using one SMA wire with bigger diameter, bundled SMA wires with smaller diameter is an excellent solution. As a result of bundling SMA wires, the capability of appliying high payload is achieved, as well.

At the end, designing a PID controller to see closed loop controlled behavior of the wires and to compare it with open loop results is the main goal of this research. Effect of bundling and of the load will be evaluated and frequency responses will be plotted to see the outcomes.

1.2 Literature Review

After Arne Ölander, Swedish physicist, first discovered SMA composed of gold-cadmium (Au-Cd), in 1932 [21], there were many scientist worked on it. Another cornerstone is discovery of Nickel-Titanium alloy called NiTiNOL by Naval Ordnance Laboratory in USA in 1962. NiTi alloy' mechanical properties are quite compatible with conventional sensors and actuators [1].

Briefly, relating SMA applications can be devided into two main cathegories based on their primary function such as generating motion or foce and deformation energy storage.

1.2.1 Biomedical applications

Since discovery of SMA, after its introduction to biomedical area, it allowed a significant progress into minimally invasive surgery (MIS) [24].

The stress-strain behaviour of SMA is quite similar to human bone and tendons, which makes SMA an excellent candidate for biomedical applications, especially stenting operations because of its simplicity of placing it in human body, shown in figure 1.2. SMA stents are easy to bend in the vessels, which are first produced by Dotter's group in 1983 [7] and its usage spreaded out to other sections of human body [24].

Figure 1.2 : Biomedical aplications of SMA respectively: braces, stamps, spine, stents, simon filter [9, 19, 20, 22, 24].

As it can be seen from the figure 1.3 and 1.4, their structure and stress-strain relation is quite similar, as well. Additionally, there are many similarities between SMA wire and muscle such as noise free working and flexibility [29].
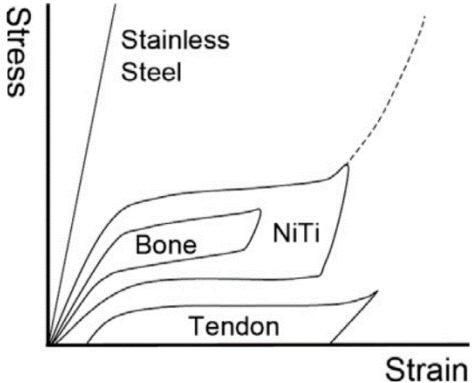

Figure 1.3 : The stress-strain relation of SMA, bone and tendons [20].

4

Artificial muscle is another human body part, which is rather convenient for using SMA wires. Because of conventional actuators' large volume, low power density and noisy working, it is hard to imitate a muscle with them. SMA wires with self-sensing capability, without using additional position sensors, it is feasible to imitate artificial muscle.
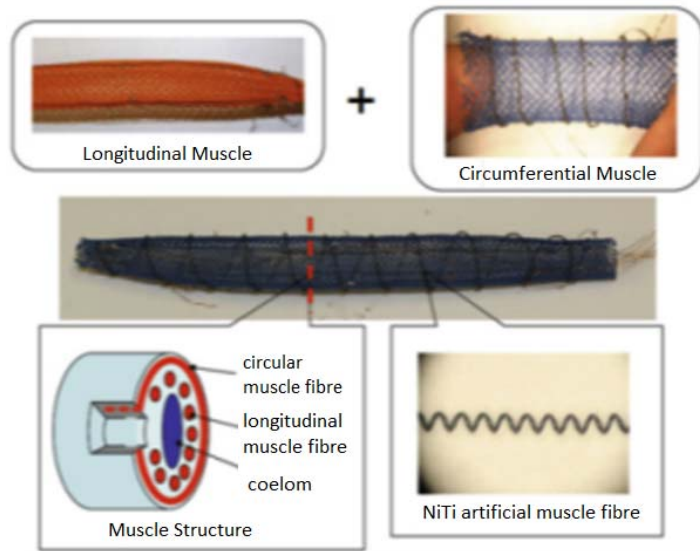

Figure 1.4 : Earth worm-like prototype and muscle structure [15,25]

1.2.2 Robotic applications

After discovery of SMA, it is used in wide range of robotic applications especially as biologically inspired artificial muscles and micro actuators [2, 5, 6, 11, 12, 16, 17].

One of the common application is finger actuator used at prosthetic hands [3]. Two SMA actuator used for actuation of the fingers by sending PWM pulses. Lara humanoid robot [33] includes 34 SMA actuator. Its gripper is shown below, figure 1.5.
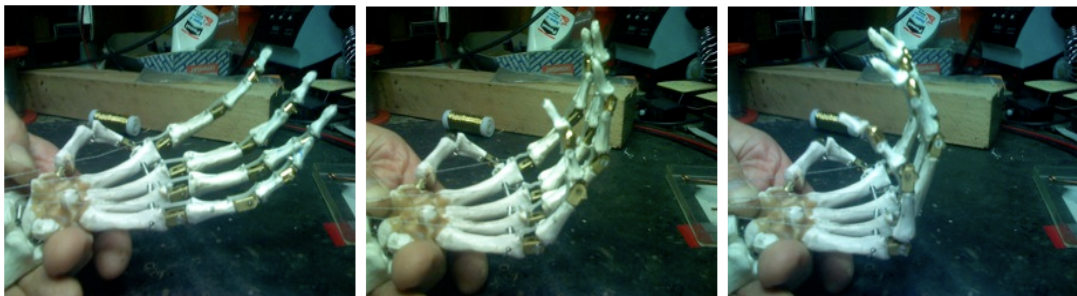

Figure 1.5 : Gripper of Lara humanoid robot [33].

In addition to grippers, legs are also actuated with SMA actuators of Lara robot, figure 1.6. Increased number of SMA wires instead of using a wider wire is useful to increase payload and to make faster the actuator.
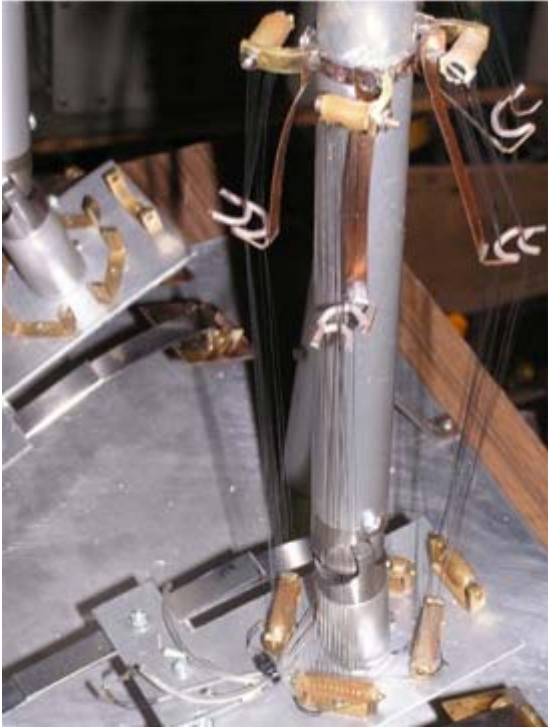

Figure 1.6 : Lara's lower leg actuators [33].

Biomimetic and humanoid robots, which are useful for exploring air, underwater and land, are categoried based on their applications such as swimmer, flier, jumper and crawler. An advanced jellyfish [26] and iTuna [23] are the aquatic robots designed by using SMA actuators, figure 1.7.
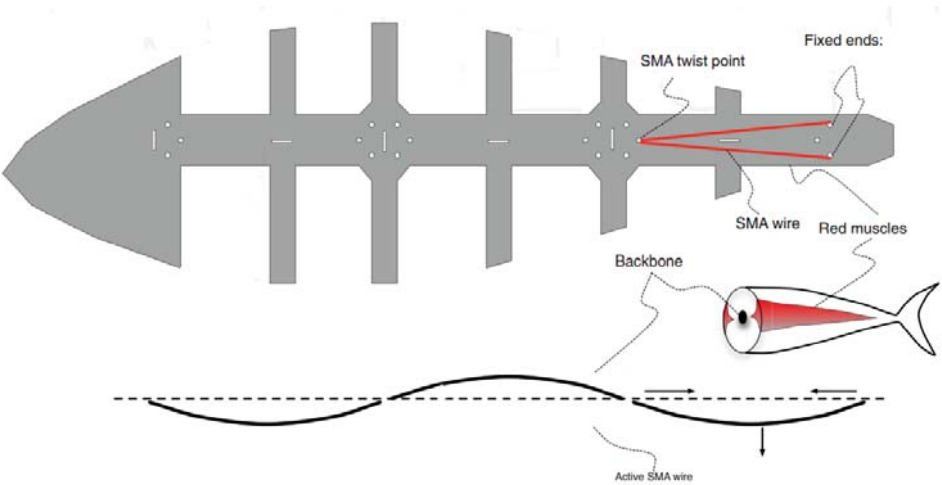

Figure 1.7 : iTuna robot fish main structure [23].

There are many flying and crawling robots actuated with SMAs. BionicOpter developed by Festo and inspired by dragonfly flight, shown in figure 1.8. Four SMA wires are used for side to side head movements and up and down tail movements in order to flight manoeuvre and stability [30, 14].

Figure 1.8 : Festo BionicOpter

Flexible muscles of BionicOpter are made of shape memory alloys. It is 175 gr with 13 degree of freedom. 8 servo motors are used for wing actuation and 4 shape memory alloys are used as head and body actuators. Beat frequency is between 15 hz and 20 hz.

2. EXPERIMENTAL SETUP

2.1 Architecture

Main architecture of the setup is shown below.

Figure 2.1 : Architecture of the setup

Mechanical and electrical parts are shown below. Only two of the printed circuit boards seen in the figure 2.2 are used to drive SMA wires.
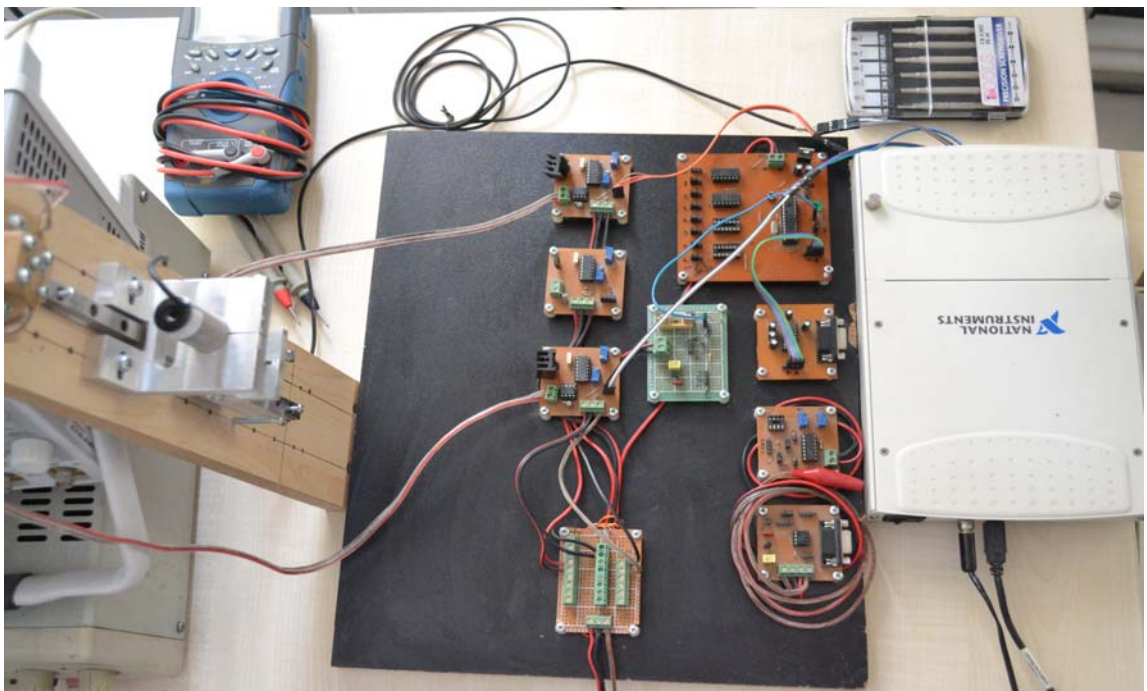

Figure 2.2 : Overall experimental setup

Briefly, a computer sends the referans position command as a voltage value via data acquisition card to SMA wire driver. SMA wire driver receives the referans voltage value then transforms it to a current value. Current flows throughout the SMA wire

and causes it to heat up. Heated SMA wire will be strained and makes the load which is hanged at the bottom of the SMA wire to displace. When it is cooled, load goes to previous position and SMA is ready to be activated again.

2.2 Overview

Main componenents of the experimental setup is shown in figure 2.3. LabView software runs in the computer and controls load's position, which means actually strain of the SMA wire. Self-sensing method is applied within LabVIEW, as well.

Data acquisition card, as the name implies, acquires data from the computer and transmits it to the SMA wire driver, and vice versa.

SMA wire driver heats up SMA wire by making flow the current throughout the wire based on the referans data received from DAQ card. On the other hand, driver sends back to DAQ card the data of voltage decrease on the wire. LabVIEW gets the value and calculates the current flowing in it.
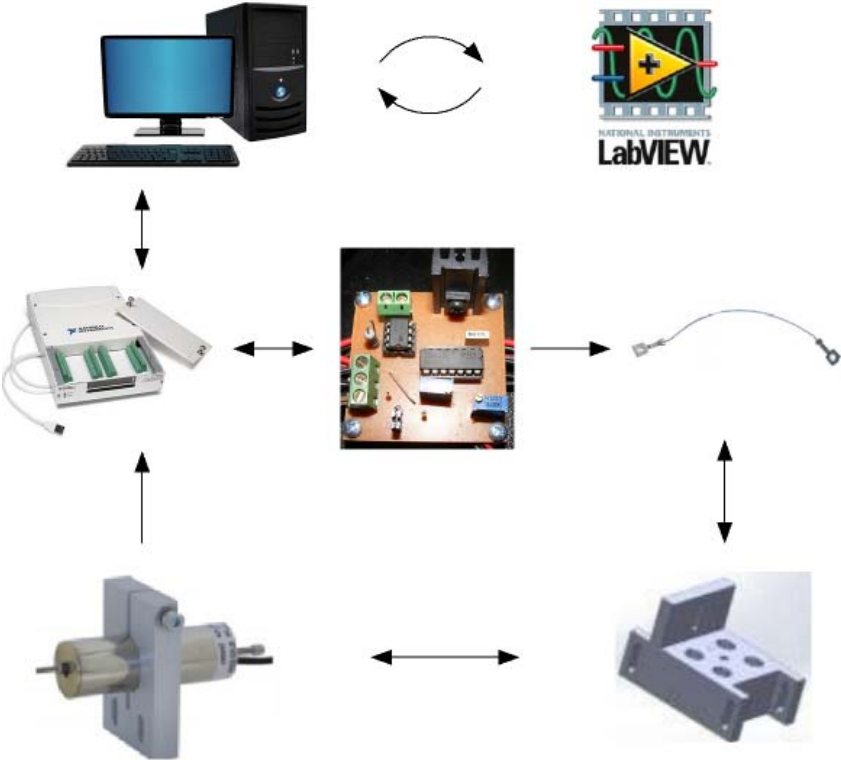

Figure 2.3 : Main components of the experimental setup

2.3 Test Bench

Test bench, shown in figure 2.4, consists of SMA wires lifting a payload (150 gr) and a LVDT (Linear Variable Differential Transformer) to measure displacement of load. Load is mounted on a vertical linear guide and core of LVDT is placed on load. When SMA wire is actuated, it causes the load to displace which in turn leads to core displacement so that LVDT can measure and sends the position data to DAQ card without using wire driver.
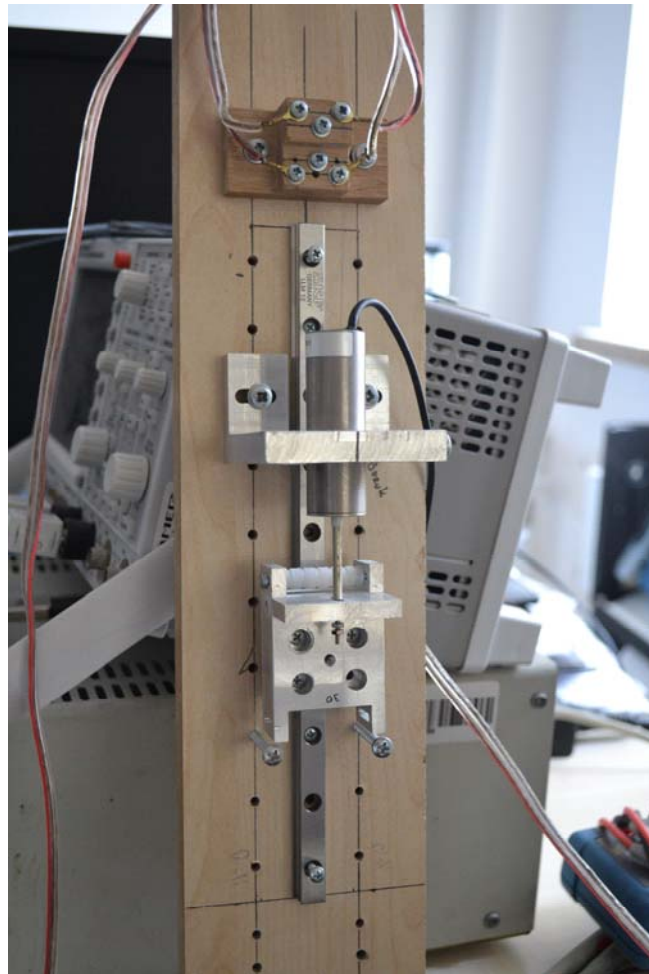

Figure 2.4 : Test bench

Respectively, two SMA wires with 76 μm diameter, one wire with 100 μm diameter and one wire with 150 μm diameter is screwed carrying same load, 150 gr. Wire length is same for three wires, 30 cm.

Mechanically parallel bundled SMA wires are more effective than one wire bundled using pulleys, that is, mechanically serial mounted. Since, in case of a damage of a wire does not make the whole actuator or muscle out of use.

2.4 Hardware Architecture

Electrical part, shown in figure 2.5, consists of two SMA wire drivers, which were built during the first phase of the study [27] and a data acquisition card (DAQ).
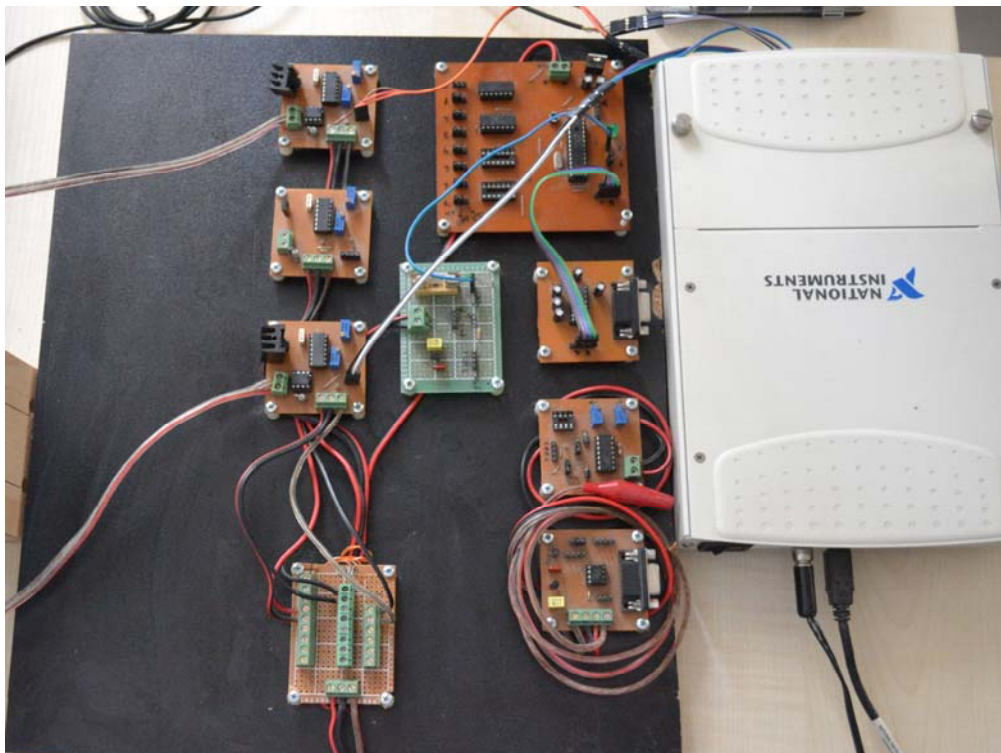

Figure 2.5 : Electrical hardware

Wire driver is responsible from sending current to the SMA wire based on the reference voltage received from DAQ card. In order the current to follow the reference value, a PI control was implemented. Controller gains are defined to provide 1 amperes output in return for a 10 volts input. The driver has a closed loop so the output, which is SMA wire actuation current, that follow the reference. However, the loop is closed within the driver and it is not sending back any current feedback to software. Instead, wire driver sends voltage drop value on the SMA wire to data acquisition card as a feedback. Since current value is already known, which is 1/10 of the reference value, it is easy to calculate wire resistance in software by dividing voltage drop value to current value. DAQ card is responsible from acquiring

reference voltage data from software and send them to SMA wire drivers. In addition, it delivers voltage drop value from driver card to software.

Mechanically parallel, electrically serial wires are effective to keep current value same but it increases or doubles the voltage value since resistance is increasing. Doubled voltage value is not in the range of driver that is why electrically serial connection of the wires is not preferred.

On the other hand, mechanically parallel and electrically parallel wires provide same voltage value but a doubled current value. In this work, it is not preferred to increase current value of one SMA wire driver to avoid heating up the transistor, which is flowing current to SMA a lot. Bearing in mind these circumstances, one wire driver is used per wire.

2.5 Software Architecture

Software part built within LabVIEW, using graphical interface. LabVIEW files are called Virtual Instrument (VI). Every VI of LabVIEW is compromised of a front panel where user interface is defined and a block diagram where the code is defined. In order to navigate between front panel and block diagram, double clicking any of the components shows the corresponding item on the block diagram [32]. Analog inputs and outputs of LabVIEW software are shown in figure 2.6.
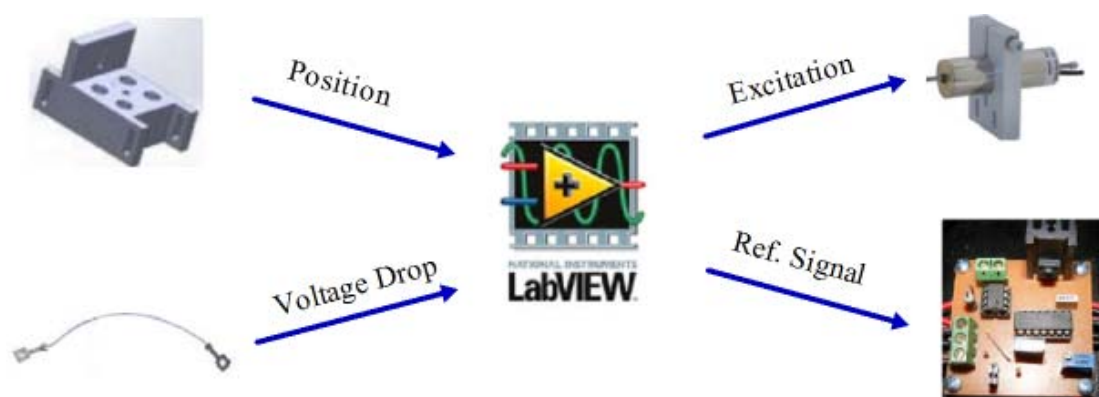

Figure 2.6 : Analog inputs and outputs of the software.

The most important feature of LabVIEW is to allow programmer to run parallel loops. Parallelism has a significant importance for breaking up applications into sub sections to execute independently. As a result, in turn, multitasking and multithreading is not complicated. In contrast, conventional text based languages require creation and managing of threads in order to run simultaneously [32].

Taking advantage of simple multitasking property of LabVIEW, four responsibility of the software part are accomplished simultaneously by using two analog outputs: powering up LVDT and sending reference voltage value to the SMA wire driver via DAQ card and two analog inputs: reading position and voltage drop on SMA wire. Front panel and block diagram views of the computer software built in LabVIEW and used for open loop experiments is shown in figure 2.7 and 2.8.
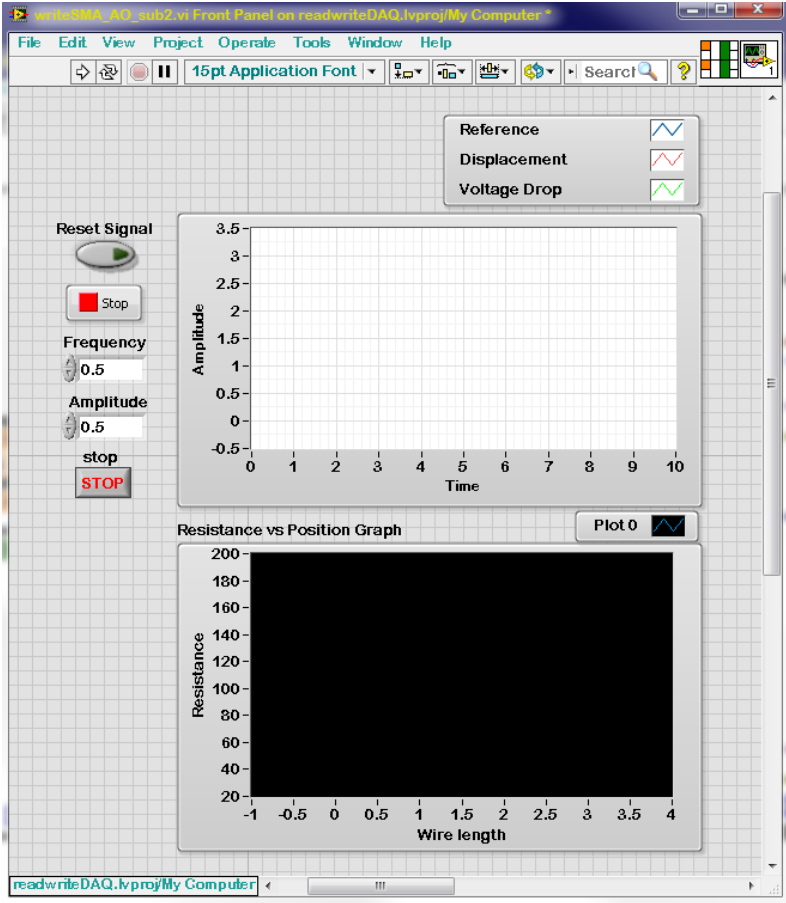

Figure 2.7 : Software front panel

By utilizing analog inputs and outputs, sine wave signal at different frequencies (between 0.1 Hz and 7 Hz) is sent as reference signal to the driver. And Bode graph is plotted for three wires with different diameter to compare their frequency responses.
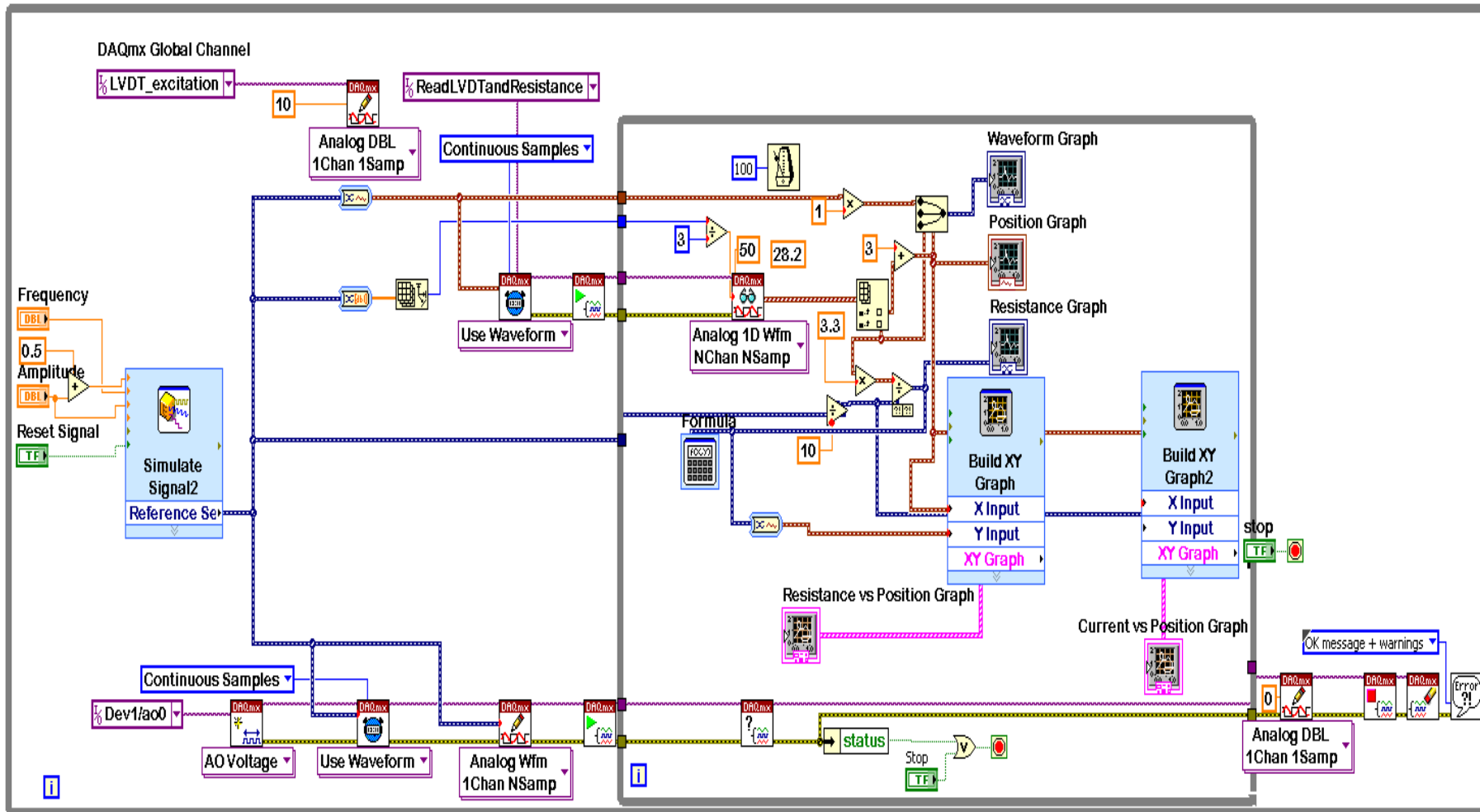
Figure 2.8 : Software block diagram.

3. FREQUENCY RESPONSE ANALYSIS

3.1 Open Loop Experiments

Measurements are carried out for three wires with different diameters and results are compared. Tests are accomplished in open loop to see pure wire frequency response without any effect of a controller. Reference signal for the current value is sent to SMA driver and position value is acquired from LVDT.

As mentioned before, sine and square wave signals at different frequencies (between 0.1 Hz and 7 Hz) are transmitted as reference signal to the driver. And Bode graph of three wires with different diameter is plotted to compare their frequency responses. For each wire, input signal magnitudes are chosen based on the approximate current value for 1 second given in the manufacturer website.

Current value is closed loop controlled within the driver with a PI controller. However, it can be assumed as open loop since there is no controller applied for position, which is the key value for frequency response. Frequency reponse analysis is the indicator of phase delay of output signal and relative magnitude based on an input signal at different frequencies in the range of interest. The point of such measurements is to have a foresight about reaction of the system to input signals at a range of frequency. Frequency responses of the system is figured with magnitudes in absolute units and phase delays in degrees. It is meant by absolute units that the ratio between input reference signal and output displacement is scaled between 0 and 1.

It can be easily observable from phase delay mentioned in frequency response how late SMA wire response is and that is the key point indicating how fast the actuator will be ready for another actuation with the same payload lifting capability with a wider wire.

3.1.1 Frequency response of SMA wire 76 μm diameter

Two wires are used with about 30 cm length to displace the load vertically. Sine wave signal at a range of frequencies between 0.1 and 7 Hertz is transmitted to driver in order to obtain frequency response of the wires.

Load displacement carried by two parallel 76 μm SMA wires is plotted below at 0.4 Hertz. Additionally, other physical behaviour of the bundle is plotted at figure 3.8. Delay is 180 degrees at 5 hertz and displacement is 0.12 mm.

Load displacement, shown in figure 3.1, is about 5 mm in case of using two parallel 76 μm diameter SMA wires in return for a sine wave signal with maximum 150 mA input current.Actually, reference value sent from software is between 0.5 and 1.5 mV. Minimum value is set to 0.5 mV so that resistance value can still be calculated by using voltage drop value on SMA wire.
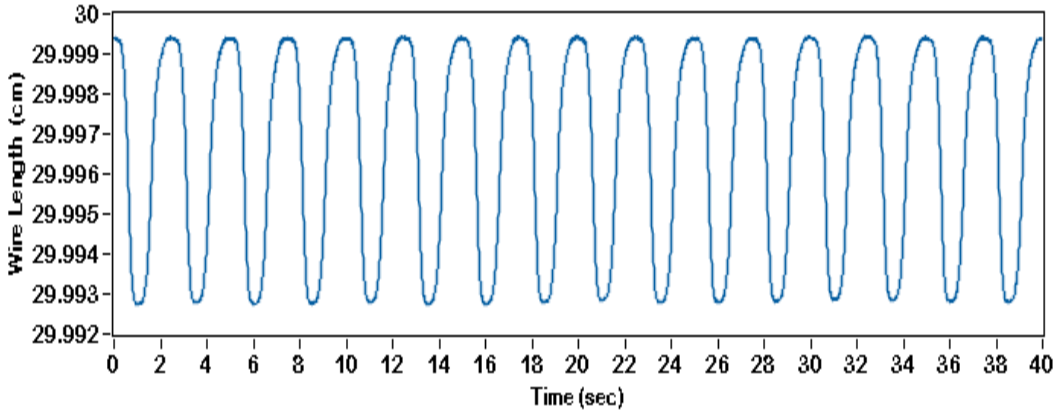

Figure 3.1 : Load displacement carried by two parallel 76 μm SMA wires.

Current value is obtained from reference value transmitted to driver by dividing it to ten since there is a 1:10 ratio between current and reference voltage value. Resistance value, as mentioned before, is calculated by dividing voltage drop value on SMA wire to current value flowing through it.

Frequency response of SMA wire 76 μm diameter is shown at Figure 3.2. Maximum displacement is 4.3 mm. At even 1 Hertz, which is relatively high frequency for SMA applications, displacement is about 1.6 mm with a delay less than 80 degrees. At 5 Hertz, it displace 0.07 mm with about 180 degrees of delay.

Pre-strain is about 1% and making the load heavier increases the strain. Displacement could also be decreased with a lighter load. So, it might be proper to use maximum payload capability to get a relatively long displacement.
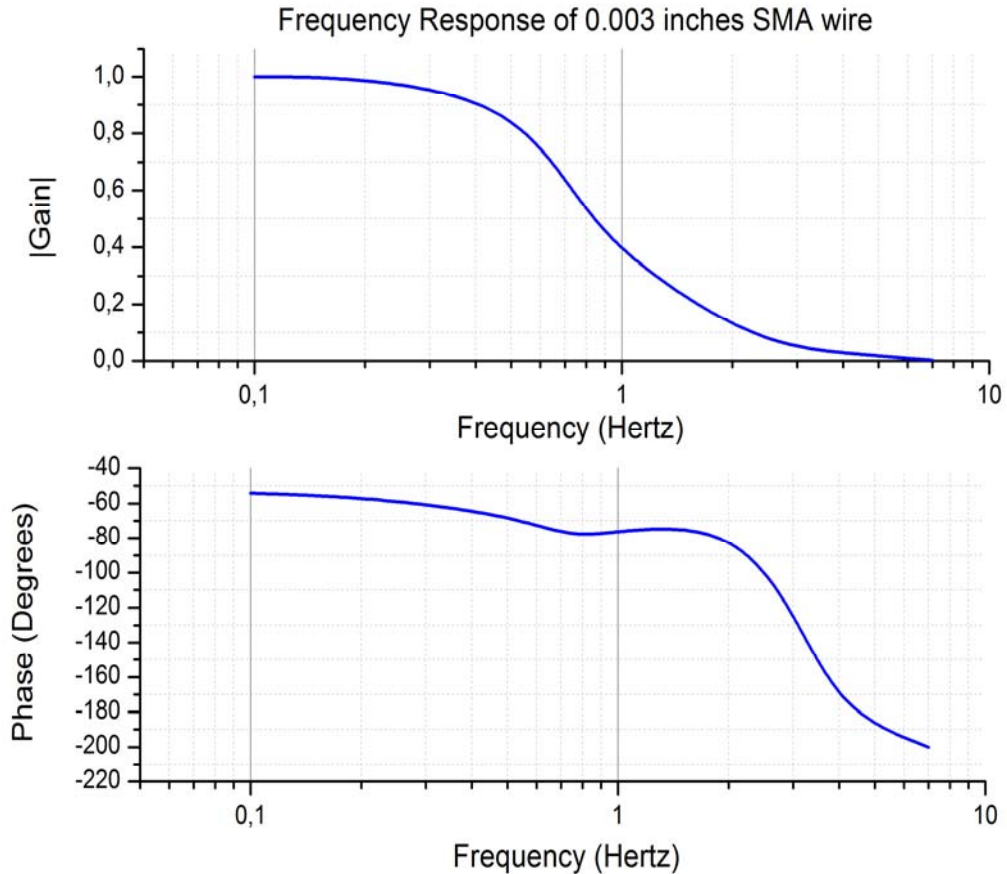
Figure 3.2 : Open loop frequency response of 0.003 inches (76 μm) SMA wire.

3.1.2 Frequency response of SMA wire 100 μm diameter

As it can be seen from the figure 3.3, frequency response of 100 μm wire is similar to 76 μm one. At low frequencies such as 0.1 Hertz, wider wire displaces longer about 0.6 mm with smaller phase delays. However, increasing the frequency of input signal drastically reduces the displacement of the load.

Even 0.24 μm increase of the diameter of the wire results in a noticeable change in test results. A delay about 180 degree occurs at 4 hertz with 0.12 mm displacement for thin wire and at 2 Hertz with 0.2 mm displacement for the thick wire. Maximum displacement of the load is 5.3 mm in return of 250 mA actuation current. Slope of the absolute gain is deeper than 76 μm wire. When it comes to 1 hertz, absolute gain becomes 0.1 for the 100 μm wire and 0.4 for the 76 μm wire.
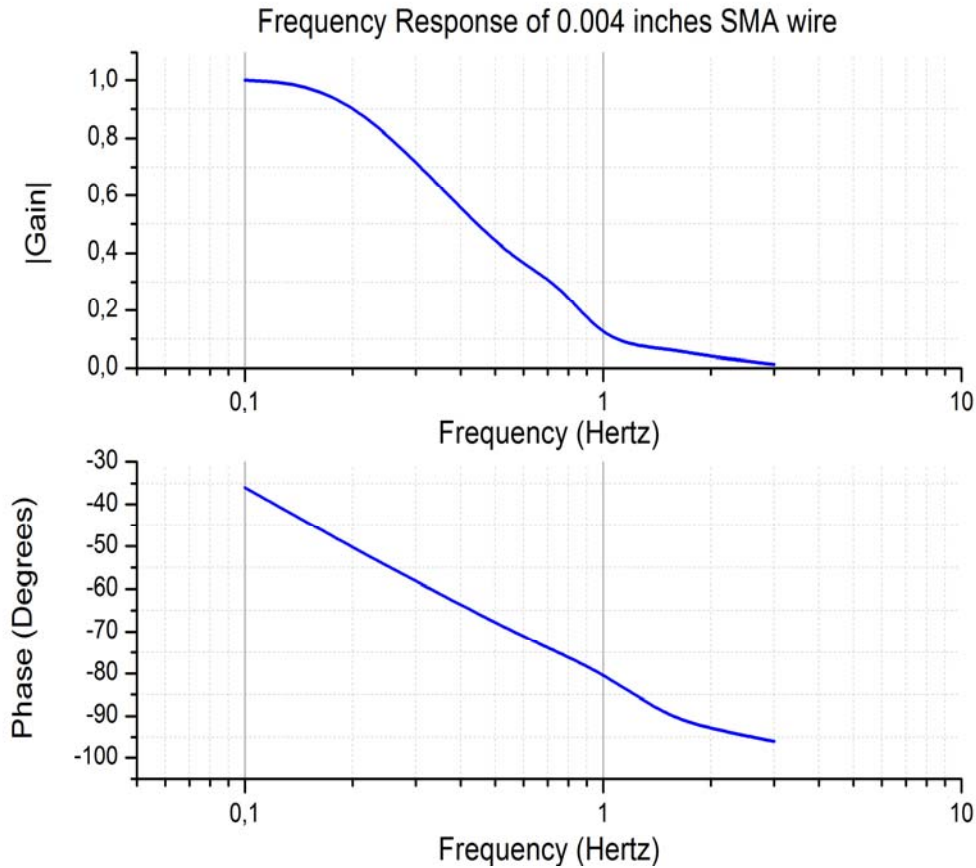
Figure 3.3 : Open loop frequency response of 0.004 inches (100 μm) SMA wire.

3.1.3 Frequency response of SMA wire 150 μm diameter

Frequency response of 150 μm SMA wire is shown in Figure 3.4. Since, weight lifting capacity of 150 μm SMA wire is higher than the applied load, displacement is less than expected. Maximum displacement is 3.1 mm in return for 300 mA actuation current. At 0.2 Hertz displacement becomes 0.8 mm, however in case of a heavier load it becomes 1.6 mm. Therefore, measured displacements are dependent on the load. Increased load weights ends up with longer displacements but bigger delays and probably shorter life expectancy.

As it is seen from the figure 3.4, the absolute magnitude of the ratio of input signal and output displacement becomes significantly small even after 0.3 hertz. Low frequencies are more fitting for thicker wires serving more payload capability, but they come with a narrower frequency range, as it is seen from the results.
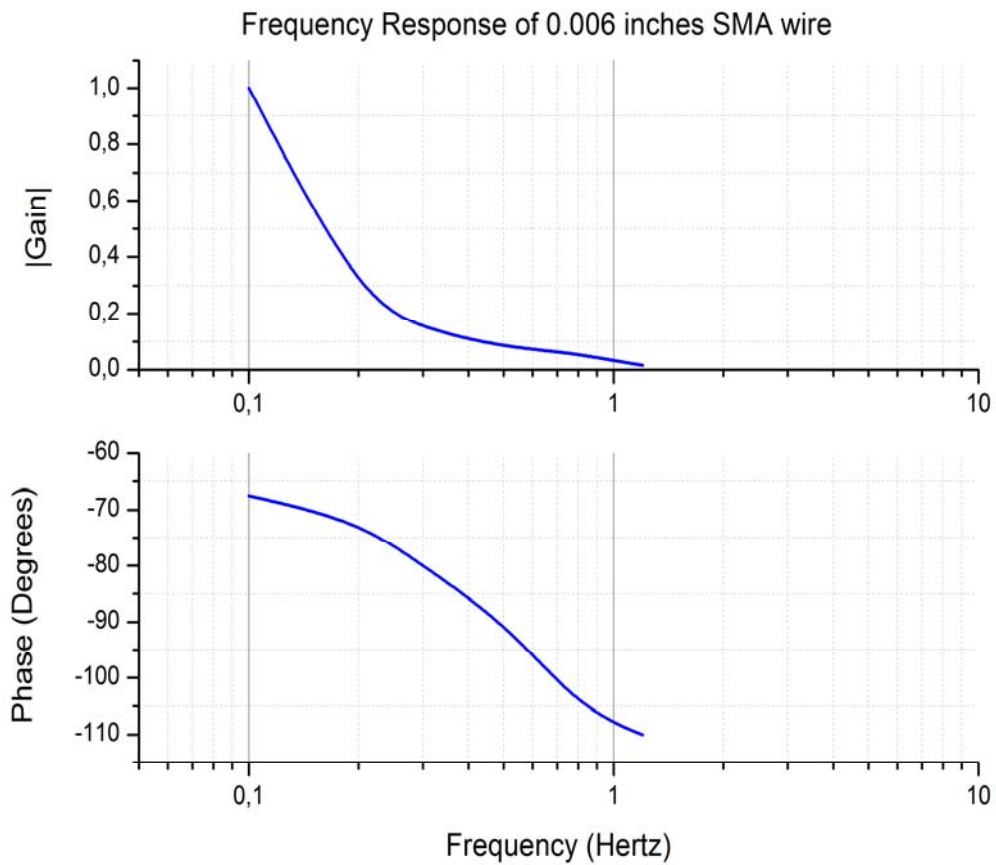
Figure 3.4 : Open loop frequency response of 0.006 inches (150 μm) SMA wire.

3.1.4 Comparison

Based on the absolute gain plots of the wires with three different diameters, shown in figure 3.5, maximum displacement is accomplished by 100 μm wire in return for maximum 250 mA contraction current. However, a fast decrease occurs in the load displacement connected to 100 μm wire at increased frequencies. 150 μm wire has the smallest contraction, probably due to the fact that, lifted load is so light than the weight it could carry.

By evaluating phase responses of the wires, it can be deduced that, 76 μm wires and 100 μm wire has almost similar phase delays, 100 μm wire acts a little bit earlier. On the other hand, 150 μm wire is the slowest one in these three wires. Thickest wire is almost two times slower than thinner wires at 1 hertz.
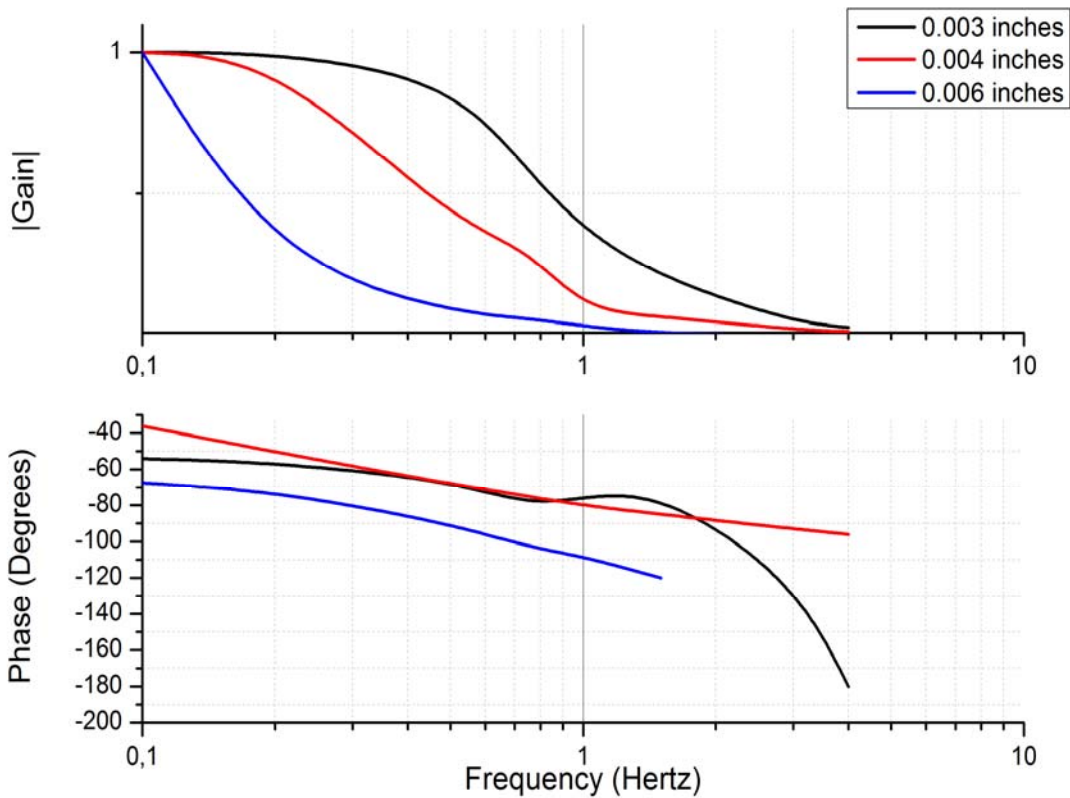
Figure 3.5 : Open loop frequency response of all three SMA wires.

3.1.5 Resistance vs position relation

Resistance versus position graph is plotted at figure 3.6. The relation is almost linear. Cooling and heating plot different lines. The gap between heating and cooling is caused by hysteresis behavior of the wire.

Increasing actuation current heats the wire and displacement. Since the temperature increased, resistance value decreases. There is an inverse proportion between position and resistance values.

In some applications, especially biomedical applications such as artificial muscle, it is hard to place the wires to the body. Besides, it is even harder to mount position sensor to measure the displacement of the muscle. In order to solve this problem, it could be feasible to establish a relation between resistance and position by using a position sensor before mounting the muscle. Acquiring the graph might be useful to

get the relation by employing Matlab polyfit function. Next step is removing the position sensor. And calculating resistance value within SMA wire driver gives also position information by using established relationship. And taking advantage of this relation, position could be calculated without using a position sensor. Based on the researches in literature [18, 28], mentioned method has the error between calculated and measured position data is less than 5%.
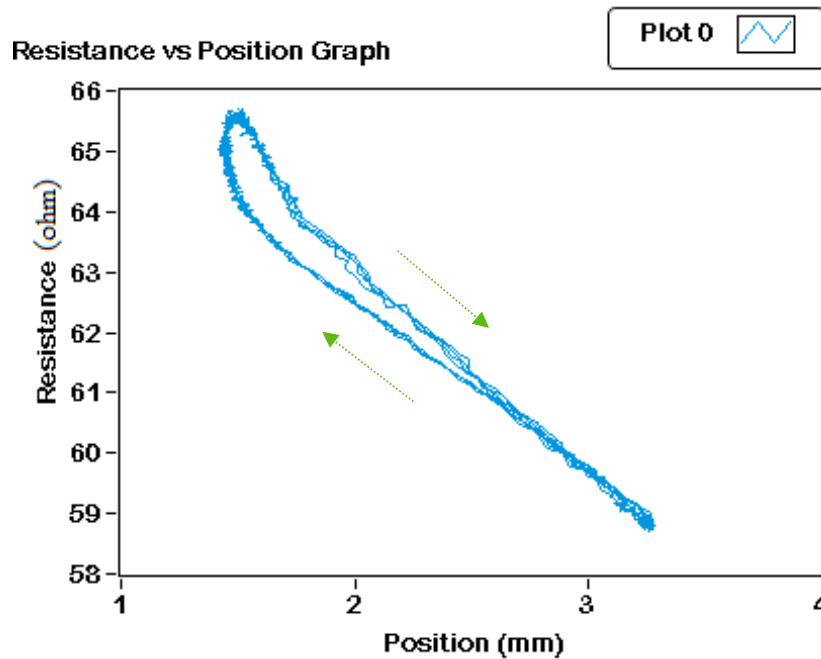

Figure 3.6 : Resistance vs position graph of two SMA wires at 0.5 hertz.

3.1.6 Current vs position relation

When current reaches the actuation current value, which is mentioned in the table A.1, given by the manufacturer, position starts to change. After this value, load is at almost standstill.

Two SMA wires are connected in parallel and actuated by a sine signal at 0.5 hertz. Actuation current versus load displacement graph is shown figure 3.7. After actuation current level, the wire starts to heat up and then position of the load changes. When the maximum position change occurs then current level decreases and the wire goes cooling cycle. And finally, wire enters its martensite form and load goes back its former position.
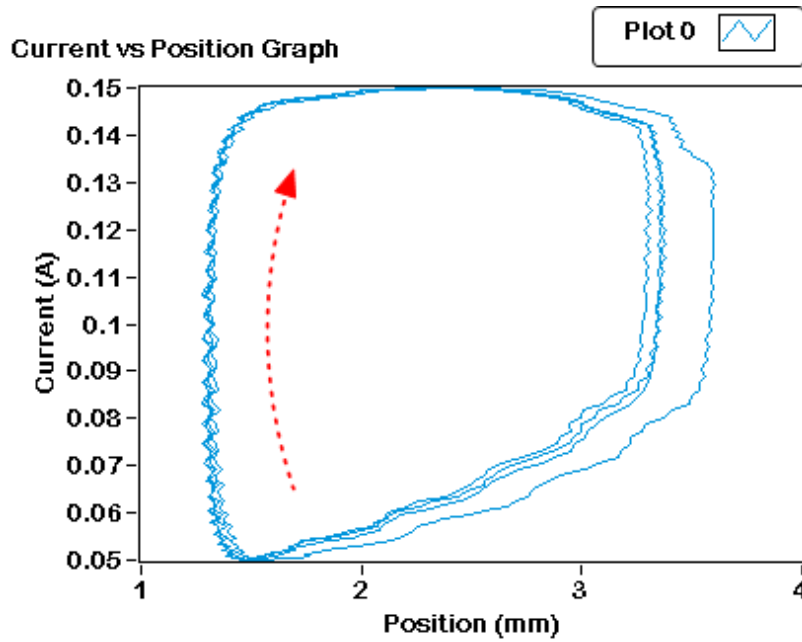
Figure 3.7 : Current vs position graph of two SMA wires at 0.5 hertz.

3.1.7 Current and position relation

Sine wave actuation current, regarding position and resistance is plotted with respect to time. As it is seen, they all similar waves with a delay in position signal since it takes time to heat up the wire. It also takes time to cool it down, when the actuation signal goes to zero.

As mentioned in the frequency response part, increasing the actuation current to a quite high value such as 0.25 amperes, results in a larger delay because of heating too much causes more time to cool down. Besides, if the frequency is high, as well, then there will not be enough time for cooling. Wire will be contracted continuously and load will be at standstill. Even increasing the current higher will end up with a burned wire.

As it can be seen from the figure 3.8, without any effect of the outside conditions, repeatability of the wire is quite well. Load goes to same position for the same actuation current. Additionally, since the same actuation current delivers same voltage drop values, which means resistance value is repeatable as well in case of same actuation current values.
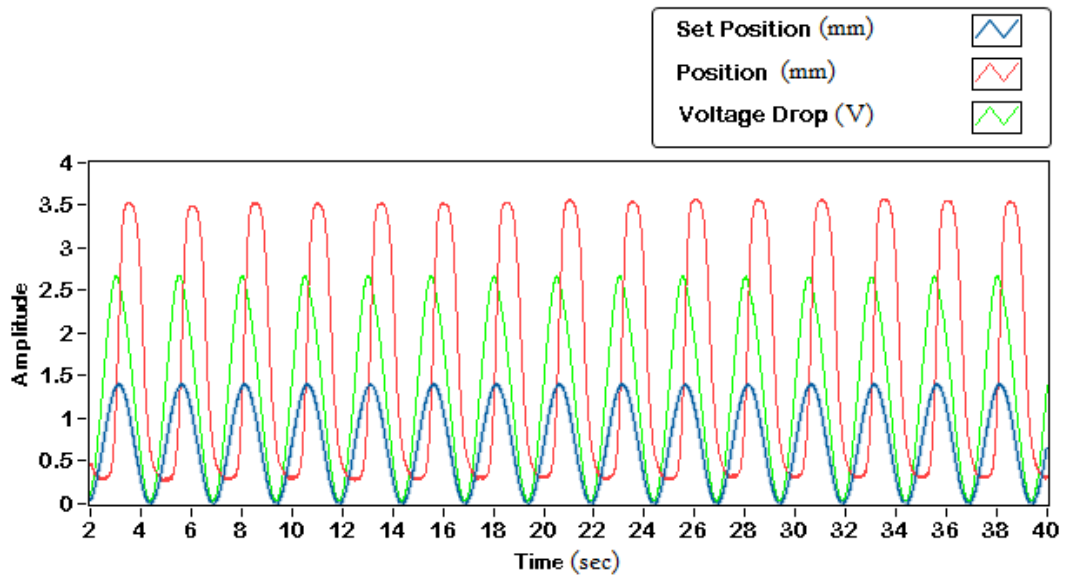
Figure 3.8 : Current and position graph of two SMA wires at 0.4 hertz.

3.2 Closed Loop Experiments

Closed loop control and analysis are carried out for three wires with different diameters and results are compared. A PID control block fed with a reference signal created current value references for PI control within the wire driver to realize an accurate positioning. Additionally, instant position value is sent back to PID control block as a feedback, shown in figure 3.9.
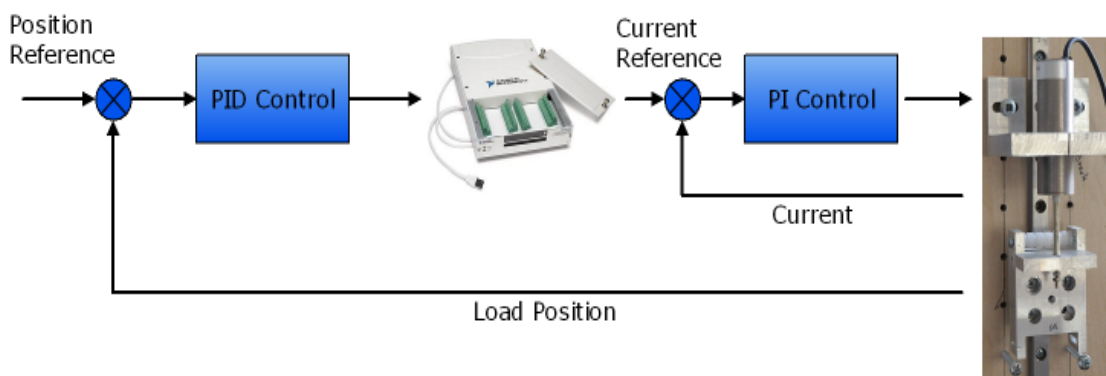

Figure 3.9 : Control system diagram of SMA wires.

Current value is closed loop controlled within the driver with a PI controller. PID control is implemented for fast and precise positioning of the load, figure 3.12. The main point of this control is to obtain the frequency response of closed loop controlled SMA wires and compare these responses with open loop results.

25

As it is accomplished with open loop experiments before, sine and square wave signals at a range of frequencies (between 0.1 Hz and 10 Hz) are transmitted as reference signal to the PID control block. And Bode graph of three wires with different diameter is plotted to compare their frequency responses.

Based on the PID controlled closed loop response of the bundled 76 μm SMA wires, shown in figure 3.10 and 3.11, response time of the bundle, which is about 0,2 second, is quite small. Overshoot is in the acceptable range.
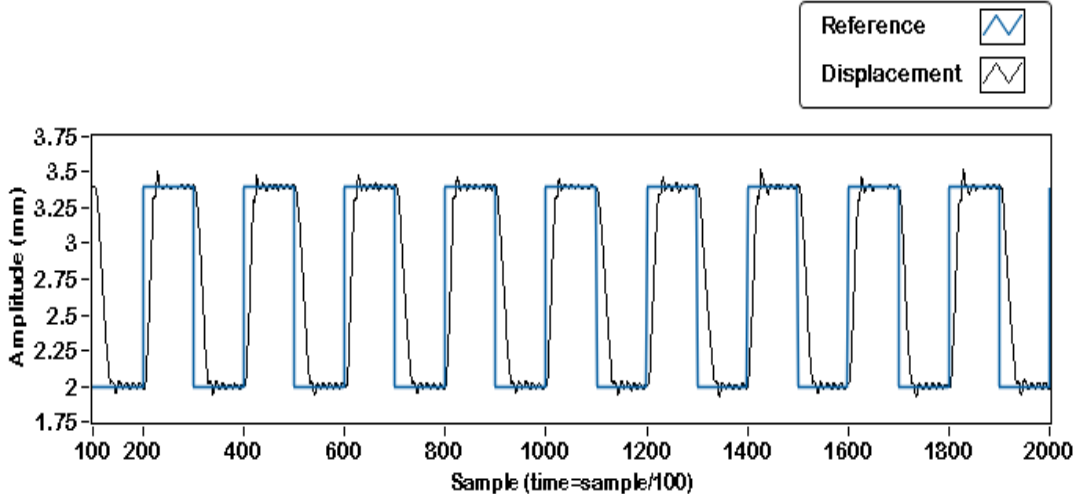

Figure 3.10 : Bundled 76 μm SMA wires position control for 20 sec at 0.5 Hz.
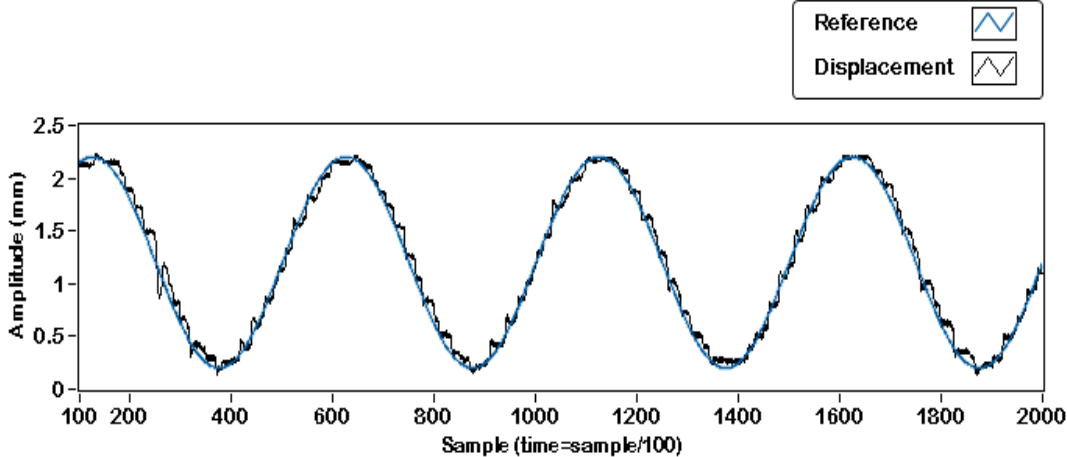
 Figure 3.11 : Bundled 76 μm SMA wires position control at 0.2 Hz carrying 163 gr.

Regarding PID controller gains, proportional control is applied for fast response time along with overshoot in case of quite high proportional gain values. Integral control is sort of prerequisite for steady state errors. PI control is not enough to remain at the current position after reaching target point.
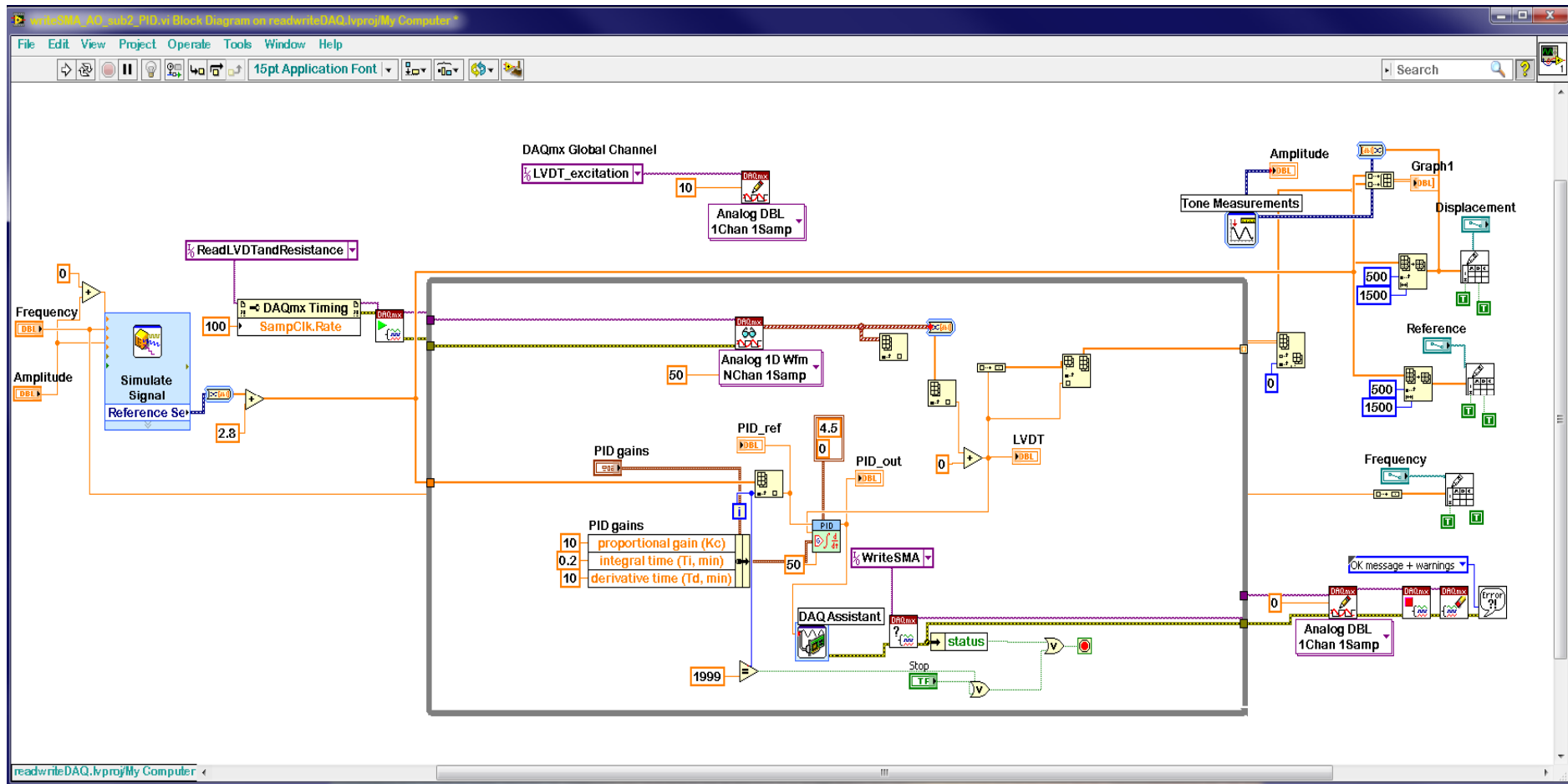
Figure 3.12 : Block diagram of PID controlled system's software.

On the response of the PI controlled system, osilations are observed. In order to eliminate these osilations around target position, derivative control is added when error is close to zero. However, derivative gain also makes the system slower. All in all, the trade-off between response time and oscillation is adjusted carefully and the gains are chosen as 10, 4 and 4 respectively.

As it can be concluded from figure 3.13 and 3.14, increased frequencies has an important effect on closed loop response of the wires.
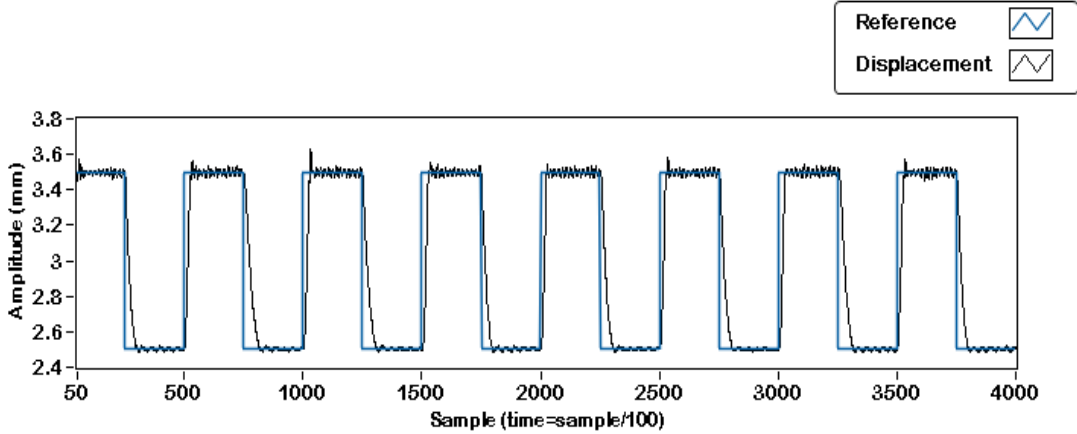

Figure 3.13 : 100 μm SMA wire position control at 0.2 Hz.

At low frequencies, it is simple for the wire to follow reference values. However, operating at high frequencies, especially for the wider wires it becomes a challenge to control the position of the wire.
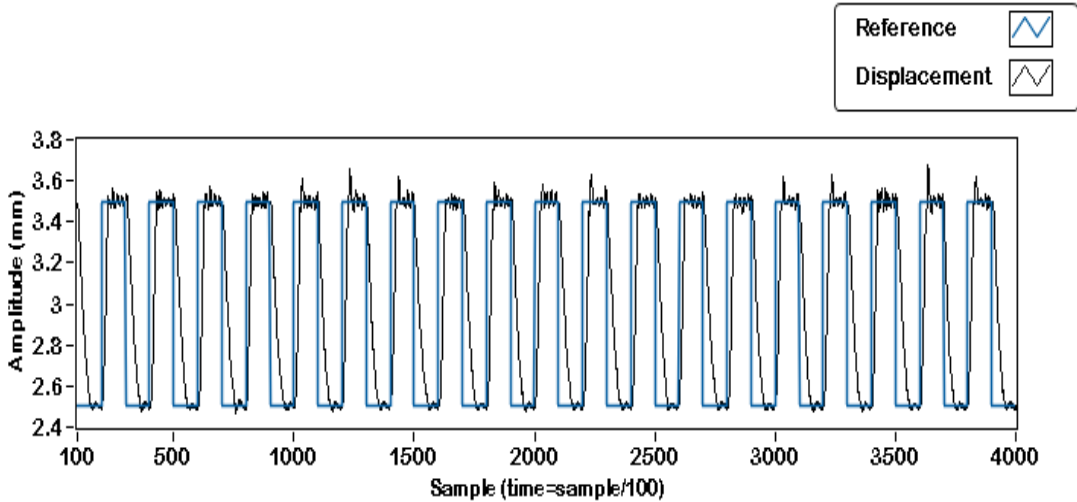

Figure 3.14 : 100 μm SMA wire position control at 0.5 Hz.

28

It can also be seen from the results that, a controller can make the system faster when heating however, it has no effect on cooling cycle. Therefore, at increased frequencies, cooling is the process that is causing the system to be slower.

Closed loop experiments have been accomplished for three different wires with about 30 cm length and carrying 150 gr load. Output of the PID block is confined with safe level of the current in order to avoid any damage either on SMA wire or on the wire driver. This current level differs from wire to wire since their actuation current levels are different. Therefore, maximum current level is modified for each SMA wires.

Bundled 76 µm wires are also tested with different payloads and responses are plotted.

3.2.1 Frequency response of SMA wire 76 µm diameter

Frequency response of the two 76 µm SMA wires is plotted at figure 3.15. The figure is essential to see the effect of the load on frequency response of the wire.
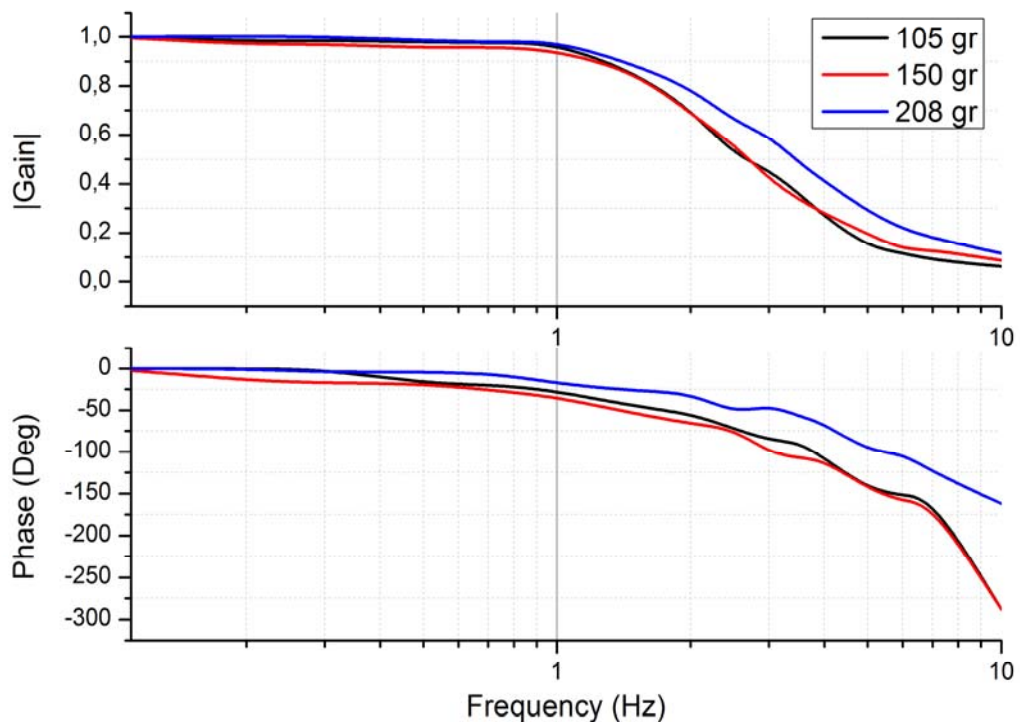

Figure 3.15 : Closed loop frequency response of bundled 76 µm SMA wires.

As it can be seen from the figure, different payloads have small effect on frequency response of the wires. The heavier the load causes small changes as longer displacement and smaller phase delay.

Closed loop controlled results of the 76 μm wire is similar to response of the 100 μm wire. Especially heating intervals of these two wires are very alike. When the increase in the diameter is very small such as 24 μm, responses are similar. However, widening more such as 50 μm the wire, after 1 Hertz, the displacement becomes very small and the difference between frequency responses becomes observable.

PID control block output is restricted within 0 – 1.8 mA. Reference and feedback signal is plotted in figure 3.11 at 0.5 hertz. In addition, for a 163 gr payload, a sine wave reference signal is fed into the PID block and the response of the wire is shown in figure 3.12 at 0.2 hertz.

3.2.2 Frequency response of SMA wire 100 μm diameter

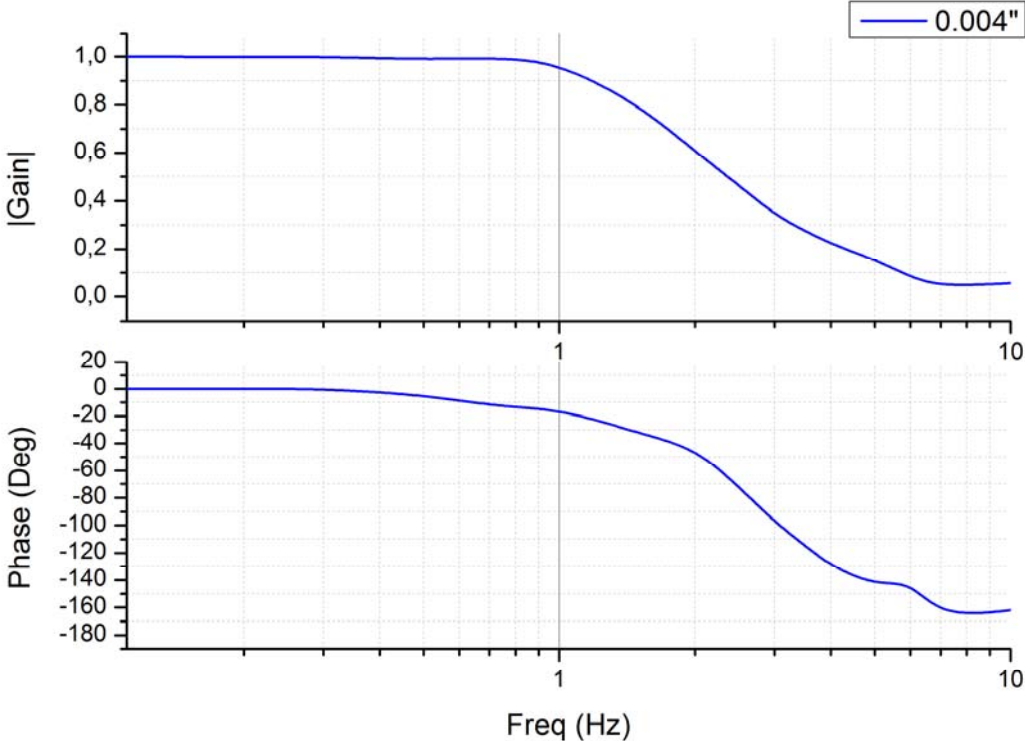Frequency response of the 100 μm SMA wire is plotted at figure 3.16.

Figure 3.16 : Frequency response of closed loop controlled 100 μm SMA wire.

As it is mentioned, it has almost same frequency response with bundle of 76 µm wires. Up to 1 Hertz, wire can follow reference signal. Displacement is close to set value, as well. Phase delay is 14 degrees and absolute gain is 0.9.

For frequencies higher than 1 hertz, it becomes challenging for 100 µm wire to track the input signal. Even at 1.5 hertz, delay almost doubles up and becomes 32 degrees and absolute gain is 0.8. The higher the frequency is, the bigger the delay gets and the the smaller distance the load displaces.

PID control block output is restricted within 0 – 2.4 mA. Reference and feedback signal is plotted in figure 3.14 at 0.5 hertz. When the figure 3.14 is compared with figure 3.11, which are responses at 0.5 hertz of 76 µm wire and 100 µm wire, wider wire has little bit more overshoot and osilation around target position. Thinner wire response at 0.5 hertz is more similar to thicker wire's response at 0.2 hertz carrying same load, 150 gr.

3.2.3 Frequency response of SMA wire 150 µm diameter

Frequency response of the 100 µm SMA wire is plotted at figure 3.17.
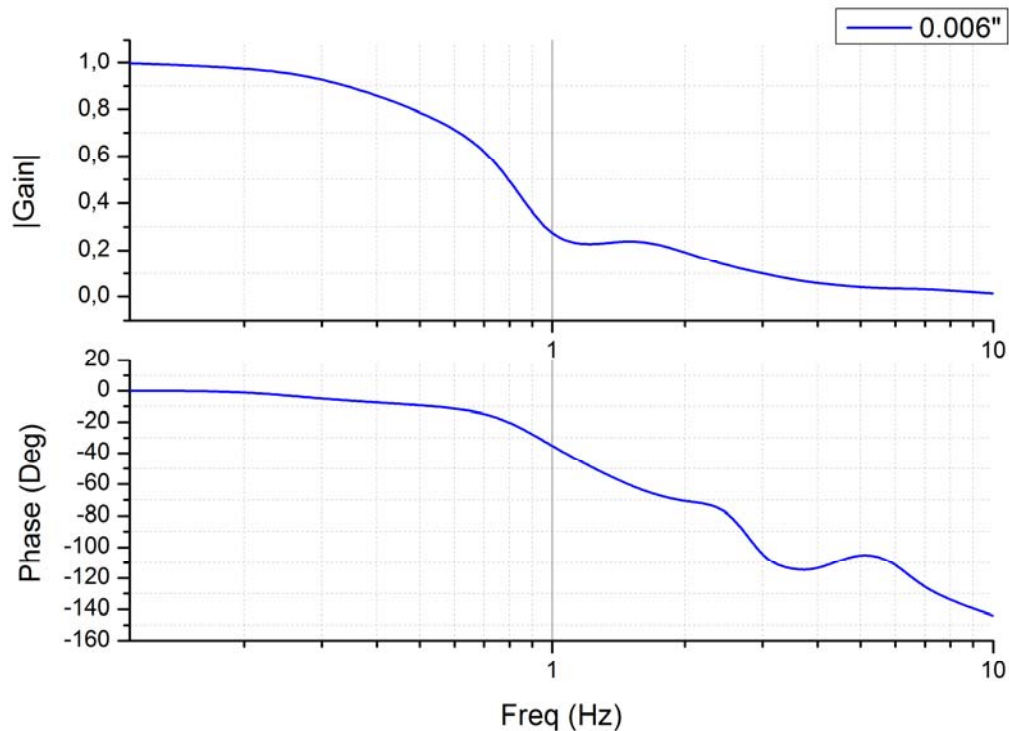
Figure 3.17 : Frequency response of closed loop controlled 150 µm SMA wire.

Phase delay of the wire is acceptable up to 1 hertz. At 0.75 hertz, delay is 15 degrees and absolute gain is 0.6. 0.25 hertz increase in frequency increases delay to 36 degrees and absolute gain becomes 0.17.

Closing the loop and controlling the wire shortened the required time for contraction of the wire. In contrast, it has no effect on cooling because of the fact that no current is flowing throughout the wire and in return PID can not affect cooling.

PID control block output is restricted within 0 – 4.2 mA. Reference and feedback signal is plotted in figure 3.18 at 0.1 hertz and figure 3.19 at 0.2 hertz.

Figure 3.18 : 150 μm SMA wire position control at 0.1 Hz.

Figure 3.19 : 150 μm SMA wire position control at 0.2 Hz.

It is clear that, even at 0.2 hertz, SMA wire is almost going back its original shape for 1 mm displacement. For higher frequencies it is harder to follow the reference signal.
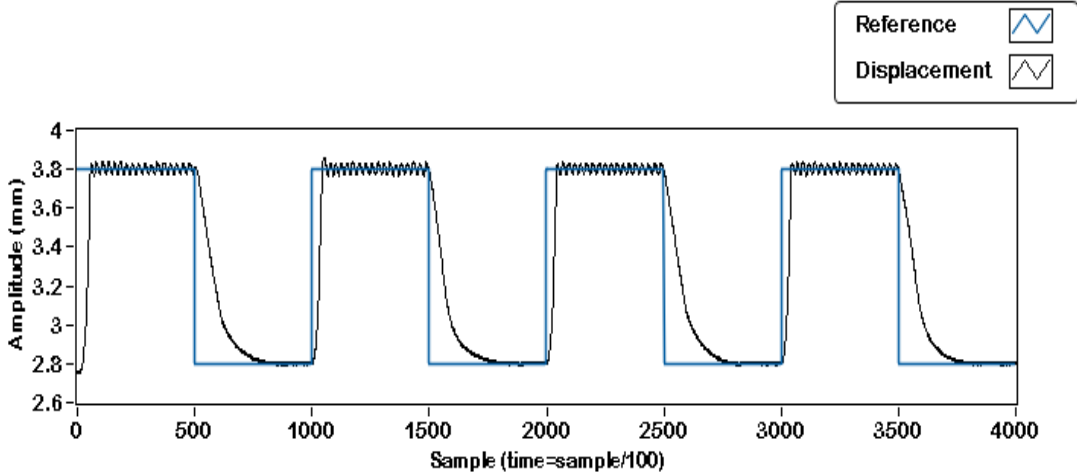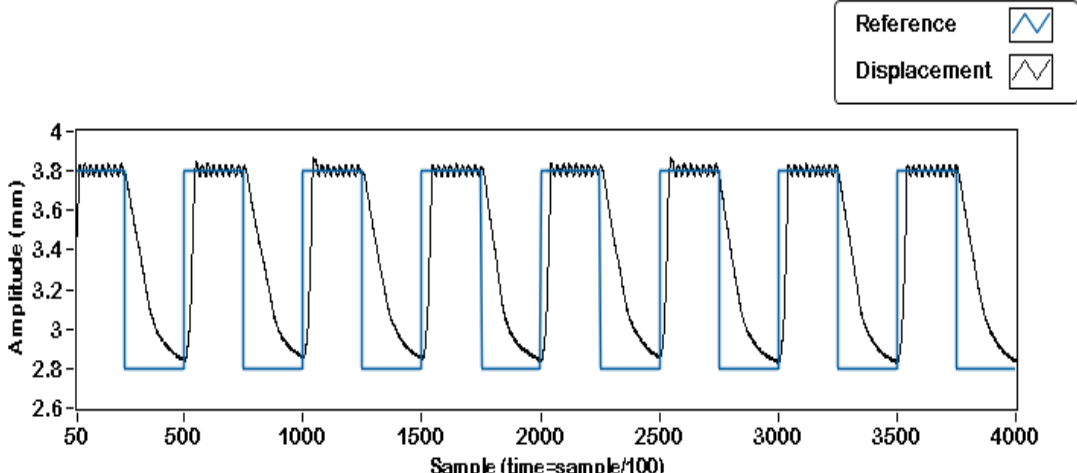
All in all, tangeble change in frequency response of the 150 μm wire occurs at about 1 hertz. But similar change occurs at 1.5 hertz for thicker wires. Widening the wire ends up with an observable delay on the response of the wire and shortening the displacement of the load.

At figure 3.20, it can be seen the response of the wire to a sine signal input at 0.5 hertz.

As it can be seen from the figure, controller sped up the wire heating time. However, it has no effect on cooling time. On the other hand, bundling has influences on both heating and cooling.
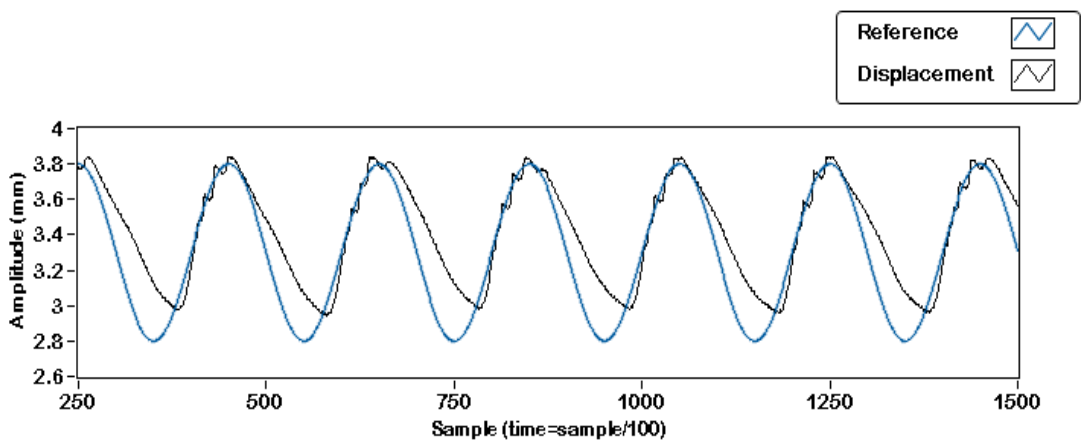
Figure 3.20 : 150 μm SMA wire closed loop position control at 0.5 Hz.

3.2.4 Comparison

Based on the closed loop controlled responses of the wires with three different diameters, as shown in the figure 3.21, closed loop control made the response of the wires quite faster. Because of the fact that, the controller first starts with maximum current to contract the wire as soon as possible, then decreases the actuation current while the error becomes smaller. Since, no current flows during cooling cycle; closed loop control has no influence on cooling.

By evaluating responses of the wires, it can be deduced that, 76 µm wires and 100 µm wire has almost similar phase delays and absolute gains. On the other hand, 150 µm wire acts similar, as well, but as a difference it makes the load displace shorter. Especially, after contraction, going back to its first position takes more time for thicker wires.

In case of small increase in diameter of the wire, bundling does not differ much but bundling instead of widening much more ends up with useful benefits especially on displacement.

Error of the controller is about 1.2 – 6.8 % at a range of frequency between 0.1-1 hz in case of bundled 76 µm SMA wires. For the same frequency range, error is between 0.98 – 3.6 % for 100 µm wire. At 0.1 – 0.5 hz, error is 0.1 – 20 % for 150 µm wire.
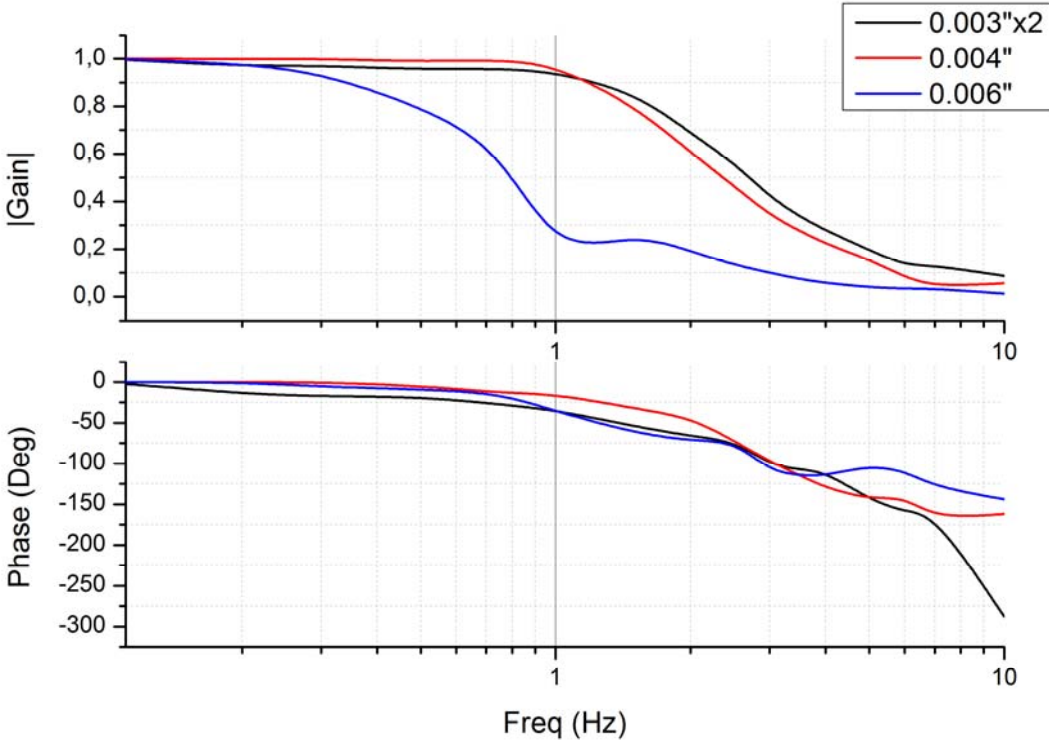

Figure 3.21 : Frequency response of closed loop controlled three SMA wires.

4. CONCLUSION AND FUTURE WORKS

4.1 Conclusion

Results of the open loop experiments show that,

- Increasing the diameter of the wire results in a slow actuation, since the wire needs more time to cool down.

- For heavier payloads, the gain is increasing which means displacement of load becomes bigger. However, as a drawback, the heavier loads lead larger delays.

- An SMA wire with 76 µm diameter can carry 80 gr load. Doubling the number of the wire increases the payload lifting capability to 160 gr which is higher than 100 µm wire's weight lifting capability. On the other hand, 76 µm wire needs 0.8 second to cool down which is 72% of cooling time of 100 µm wire and 40% cooling time of 150 µm wire. Even 24 µm widening of the wire results in about 30% slower cooling time, which is more obvious at relatively high frequencies.

- Phase delay is 180 degree at 5 Hz for 76 µm wire, 2 Hz for 100 µm wire under 150 gr loading. For the same load, 150 µm wire displaces the load 0.05 mm at 1.2 Hz. Since the wires are twofold, the variation of wire length is actually double of these displacements. Bearing mind that the narrow bandwidth of SMA wires, choosing a bigger diameter SMA results a drastically reduced bandwidth.

- For a 0.2 Hz input signal, displacement of the load, which is 150 gr, is 4.3 mm for 76 µm wire, 5 mm for 100 µm wire and 0.8 mm for 150 µm wire. Using about 300 gr payload instead of 150 gr leads 150 µm SMA wire to displace 1.6 mm instead of 0.8 mm.

- Two SMA wires with 76 µm diameters have the same payload lifting capability with one SMA wire with 100 µm diameter. In addition, as mentioned before, two 76 µm SMA wires are about 30% faster than 100 µm

SMA wire. Additionally, in theory, it requires two more SMA wires with 76 μm to have the same weight lifting capability with one SMA wire with 150 μm diameter.

- Increasing the actuation current of the wires to a quite high value such as 0.25 amperes, results in a larger delay because of heating too much causes more time to cool down.

Outcomes of the closing the control loop are;

- Controller makes the SMA wire contract faster. Since the controller first starts with maximum current to contract the wire rapidly, then decreases the actuation current while the error becomes smaller.

- Because of the fact that, no current flows during cooling cycle; closed loop control has no influence on cooling. However, bundling has influence on both heating and cooling cycles, since it could allow the wire cool down quicker.

- At 0.2 hertz, 76 μm and 100 μm wires respond to input signal with about 50 degrees of delay. 150 μm wire has a delay about 70 degrees. The closed loop control is eliminated these delays and the all three wires can follow the sine input without any delay at 0.2 hertz.

- Phase delays occuring at 0.2 hertz in case of open loop experiments takes place at about 2 hertz for the closed loop controlled experiments.

- Absolute gain is less than 0.5 for 76 μm and 100 μm wires and almost zero for 150 μm at 1 hertz. At the same frequency, it is about 1 for 76 μm and 100 μm wires and 0.3 for 150 μm at 1 hertz. It can be concluded that, closed loop control of the wires is quite beneficial for both pursuing input signal and displacement of the load.

- Bundling the wires is very effective to accelerate the response and makes evident difference in open loop experiments.

- In closed loop experiments, for small increase in diameter of the wire, bundling does not make a significant difference. However, in case of 76 μm and 150 μm wires, instead of doubling the diameter of the wire, it would be more useful, especially for longer displacement at high frequencies, to use

36

4x76 μm wires in parallel to carry the same load. Since 150 μm wire has a 320 gr payload capability and it is 80 gr for the 76 μm wire.

- Payload has an effect on displacement in open loop experiments but closed loop controlled wire is almost not affected from the load.

4.2 Future Works

Connection of the SMA wires to the workbench is quite difficult. Bundled wires should have the same length. So that, they will have an equal share of strain. So using small crimps, instead of screwing them to the workbench would make it more practical. Additionally, in case of usin SMA wires as artifical muscle or actuator, using teflon plates at two ends of the wires might be a useful solution of bundling and make easier to equally share the strain caused by the load.

Another mechanical improvement could be concealing the system from environment. Since even flowing air coming from an opened window might affect the results. Placing the system in a box, in order to avoid any influence from the environment, would be a slight but beneficial modification.

A revised SMA wire driver could be more beneficial because of the fact that it could not drive serially connected wires during experiments since it is planned to drive only one wire. That is why two driver is used to activate two wires. It could be used transistors and opamps, if necessary, with higher current level capabilities for the wires to be used as a bundle with high number of SMA wires.

Biomedical applications such as artificial muscle or micro gripper does not have enough space and making it as tiny as possible would be a quite essential improvement. On this aim, removing LVDT from the system will save relatively large space. To accomplish that, it is required to find another way of measuring position. Establishing a relation between resistance and position of the load or strain of the wire would be a major enhancement on the software part. Since the relation between them is almost linear, shown in figure 3.6, it would be a useful way of estimating position by calculation of the resistance value within software based on the data coming from SMA wire driver. Since there is a gap between cooling and heating cycles, it might be useful to establish two different relation, one for cooling and the other for heating.

REFERENCES

[1] **Buehler W.J., Gilfric J.V. and Wiley R.C.** (1963) Effect of low-temperature phase changes on the mechanical properties of alloys near composition TiNi. Applied Physics. 1963;34:1475-7.

[2] **Caldwell D.G. and Taylor P. M**. (1988) Artificial muscles as robotic actuators. In: IFAC Robot control conference. P. 401-6.

[3] **Chee S. L., Yokoi H. and Arai T.** (2005) New shape memory alloy actuator: design and application in the prostehetic hand. In: 27th Annual International Conference of the Engineering in Medicine and Biology Society (IEEE-EMBS) p. 6900-3.

[4] **Coral W., Rossi C., Colorado J., Lemus D. and Barrientos A.** (n.d.) SMA-based muscle-like actuation in biologically inspired robots: A state of the art review. http:d.doi.org/10.5772/50209.

[5] **Dilibal S., Tabanlı R. M., Dikicioğlu A**. (2004) Development of shape memory actuated ITU Robot Hand and its mine clearance compability. Journal of Materials Processing Technology, 155–156 (2004) 1390–1394.

[6] **Dilibal S., Guner E., Akturk N**. (2001) Three-finger SMA robot hand and its practical analysis. Robotica, doi: 10.1017/S0263574701003757

[7] **Dotter C.T., Buschmann R.W., McKinney M.K. and Rösch J**. (1983) Transluminal expandable nitinol coil stent grafting: preliminary report, Radiology 1983;147:259-60

[8] **Dönmez B., Özkan B. and Kadıoğlu S.** (2010). Precise position control using shape memory alloy wires, Turkish Journal of Electrical Engineering and Computer Science. Vol. 18, no. 5. doi:10.3906/elk-0906-14.

[9] **Duerig T.W., Pelton A. and Stöckel D**. (1999) An overview of nitinol medical applications. Mater Sci Eng, 1999;273-275:149-60

[10] **Duerig T.W.** (1990). Applications of shape memory, martensitic transformations, Materials Science Forum, pp. 679-692.

[11] **Fujita H.** (1989) Studies of micro actuators in Japan. In: IEEE International conference on robotic automation. Institute of Industrial Science, p. 1559-64.

[12] **Honma D. and Miwa Y.I**. (1985) Micro robots and micro mechanisms using shape memory alloy to robotic actuators. Rob Syst 1985;2:3-25

[13] **Ikuta K.** (1990). Micro/miniature shape memory alloy actuator, Proceedings of IEEE Conference on Robotics and Automation, pp. 2156-216.

[14] **Jani J.M., Leary M., Subic A., Gibson M.A.**, (2013) A review of shape memory alloy research, applications and opportunities, Materials and Design, http://dx.doi.org/10.1016/j.matdes.2013.11.084

[15] **Kim S., Hawkes E., Choy K., Joldaz M., Foleyz J. and Wood R. Micro** (2009)artificial muscle fiber using niti spring for soft robotics. In:

IEEE/RSJ İnternationa conference on intelligent robots and systems. IEEE: 2009 p. 2228-34

[16] **Kuribayashi K.** (1986) A new actuator of a joint mechanism usin TiNi alloy wire. Int J Rob Res 1986;4:47-58

[17] **Kuribayashi K.** (1989) Milimeter size joint actuator using shape memory alloy. In: Micro electro mechanical systems. Proceedings, an investigation of micro structures, sensors, actuators, machines and robots. IEEE: 139-44.

[18] **Lan C.C., Fan C.H.,** (2010) An accurate self-sensing method for the control of shape memory alloy actuated flexures, Sensors and Actuators A: Physical. Doi:10.1016/j.sna.2010.07.018

[19] **Machado L.G. and Savi M.A**. (2003) Medical applications of shape memory alloys. Braz J Med Biol Res 2003;36:683-91

[20] **Morgan N.B.** (2004) Medical shape memory alloy aplications – the market and its products. Mater Sci Eng. A 2004;378:16-23

[21] **Ölander A.** (1932) An electrochemical investigation of solid camium-gold alloys. Am Chem Soc 1932;54:3819-33.

[22] **Petrini L. and Migliavacca F**. (2011) Biomedical applications of shae memory alloys. J Metall 2011.

[23] **Rossi C., Colorado J., Coral W. and Barrientos A**. (2011). Bending continuous structures with SMAs: a novel robotic fish design, Bioinspiration biomimetics 045005(4): 045005. URL: http://iopscience.iop.org/1748-3190/6/4/045005

[24] **Song C.** (2010) History and current situation of shape memory alloys devices for minimally invasive surgery. Open Med Dev J 2010;2:24-31.

[25] **Stirling L., Yu C.H., Hawkes E., Wood R. and Goldfield E**. et al (2011) Applicability of shape memory alloy wire for an active soft orthotic. J Mater Eng Perform 2011;20:658-62

[26] **Tadesse Y., Villanueva A., Haines C., Novitski D., Baughman R. and Priya, S.** (2012). Hydrogen-fuel-powered bell segments of biomimetic jellyfish, Smart Materials and Structures 21(4): 045013.

[27] **Tağlıoğlu G. B.,** (2013) Position and speed control of shape memory alloys for usage as actuators, *PhD Thesis*, ITU.

[28] **Wang T.M., Shi Z.Y., Liu D., Ma C., Zhang Z.H.** (2012) An accurately controlled antagonistic shape memory alloy actuator with self-sensing. Sensors, ISSN 1424-8220, www.mdpi.com/journal/sensors.

[29] **Zhang J. and Yin Y.** (2012) SMA-based bionic integration design of self-sensor-actuator-structure for artificial skeletal muscle. Sensors and Actuators A: Physical.

[30] **Festo BionicOpter** (2013) - Inspired by dragonflight. Festo 2013.

[31] **Flexinol Actuator Wire Technical and Design Data** (2014) Data retrieved: 10.12.14, address: www.dynalloy.com/ tech_data_wire.php.

[32] **LabVIEW introduction** (2014) Data retrieved: 22.11.2014, address: www.ni.com.

[33] **Lara Humanoid Robot** (2006/2007) Data retrieved: 19.11.2014. Adress: http://www.thelaraproject.com/Welcome.html.

[34] **Materials forming SMA** (2014) Data retrieved: 22.11.2014, address: http://en.wikipedia.org/wiki/Shape-memory_alloy.

APPENDICES

APPENDIX A: Tables

APPENDIX A

Table A.1 : Properties of Flexinol Wires

Diameter Size inches (mm)	Resistance ohms/inch (ohms/m)	Heating Pull Force* pounds (grams)	Cooling Deform. Force* pounds (grams)	Approximate Current for 1 Second Contraction (mA)	Cooling Time 158° F, 70°C "LT"Wire** (seconds)
0.003 (0.076)	5.9 (232)	0.18 (80)	0.07 (32)	150	0.8
0.004 (0.10)	3.2 (126)	0.31 (143)	0.12 (57)	200	1.1
0.006 (0.15)	1.4 (55)	0.71 (321)	0.28 (128)	410	2

* The Heating pull force is based on 25,000 psi (172 MPa), which for many applications is the maximum safe stress for the wire. However, many applications use higher and lower stress levels. This depends on the specific conditions of a given design. The cooling deformation force is based on 10,000 psi (70 MPa), which is a good starting point in a design. However, this value can also vary depending on how the material is used.

** The contraction time is directly related to current input. The figures used here are only approximate since room temperatures, air currents, and heat sinking of specific devices varies.

*** Approximate cooling time, at room temperature in static air, using a vertical wire. The last 0.5% of deformation is not used in these approximations. LT = Low Temperature Flexinol® Actuator wire. [16]

CURRICULUM VITAE

Name Surname: Saniye Dindar

Place and Date of Birth: Kayseri, 09.08.1986

E-Mail: eylem408@gmail.com

B.Sc.: Kocaeli University, Mechatronics Engineering